

# We are IntechOpen, the world's leading publisher of Open Access books Built by scientists, for scientists

6,900

Open access books available

185,000

International authors and editors

200M

Downloads

Our authors are among the

154

Countries delivered to

TOP 1%

most cited scientists

12.2%

Contributors from top 500 universities



WEB OF SCIENCE™

Selection of our books indexed in the Book Citation Index  
in Web of Science™ Core Collection (BKCI)

Interested in publishing with us?  
Contact [book.department@intechopen.com](mailto:book.department@intechopen.com)

Numbers displayed above are based on latest data collected.  
For more information visit [www.intechopen.com](http://www.intechopen.com)



---

## Superhydrophobicity through Coatings Prepared by Chemical Methods

---

Sepehr Shadmani, Mehdi Khodaei,  
Xiuyong Chen and Hua Li

Additional information is available at the end of the chapter

<http://dx.doi.org/10.5772/intechopen.92626>

---

### Abstract

Superhydrophobic surfaces were first observed in nature like on a lotus leaf. The surfaces need to have hierarchical micro- and nanoscale roughness and low surface energy to achieve superhydrophobicity. Their unique behavior against water leads to various applications like corrosion resistance, oil-water separation, self-cleaning properties, anti-icing properties, drag reduction, and antibacterial properties. To investigate the wetting behavior of the coating, water contact angle, contact angle hysteresis and sliding angle must be measured. If WCA is higher than  $150^\circ$  and sliding angle and contact angle hysteresis are below  $10^\circ$ , then it can be concluded that the surface is superhydrophobic. Various fabrication methods including lithography, templating, chemical vapor deposition, layer-by-layer deposition, colloidal aggregation, and electrospinning and electrospraying especially wet chemical method are thoroughly studied. Among all fabrication methods, the wet chemical technique is one of the promising methods due to its low cost and capability of large-scale production and also the substrate shape and dimensions having a minimal effect on the process. Superhydrophobic coatings still lack sufficient mechanical endurance. Also, in all traditional superhydrophobic coatings, it is necessary to lower the surface energy by a low-energy polymeric material that does not have suitable bonding and stability in harsh environments.

**Keywords:** superhydrophobic, coatings, chemical synthesis, surface engineering, self-cleaning, antimicrobial

---

## 1. Definition of superhydrophobicity

### 1.1. Concept

Superhydrophobic properties were first observed in nature and on the surface of *Nelumbo nucifera* (lotus), butterfly wings, *Brassica oleracea*, *Colocasia esculenta*, etc. [1, 2]. The superhydrophobic properties appeared due to unique surface structure and low surface energy. A superhydrophobic surface repels water droplets and does not get wet in contact with water. In other words, surface behavior against water is evaluated by the water contact angle measurements which will be discussed later. On a superhydrophobic surface, WCA is higher than  $150^\circ$ , while for hydrophobic and hydrophilic surfaces, this value is, respectively,  $90^\circ$ – $150^\circ$  and below  $90^\circ$ . In **Figure 1**, some natural superhydrophobic surfaces are introduced.

Higher WCA values mean that a water droplet tends to maintain a spherical shape on the surface. On the other hand, lower WCA shows the tendency of a water droplet to spread on

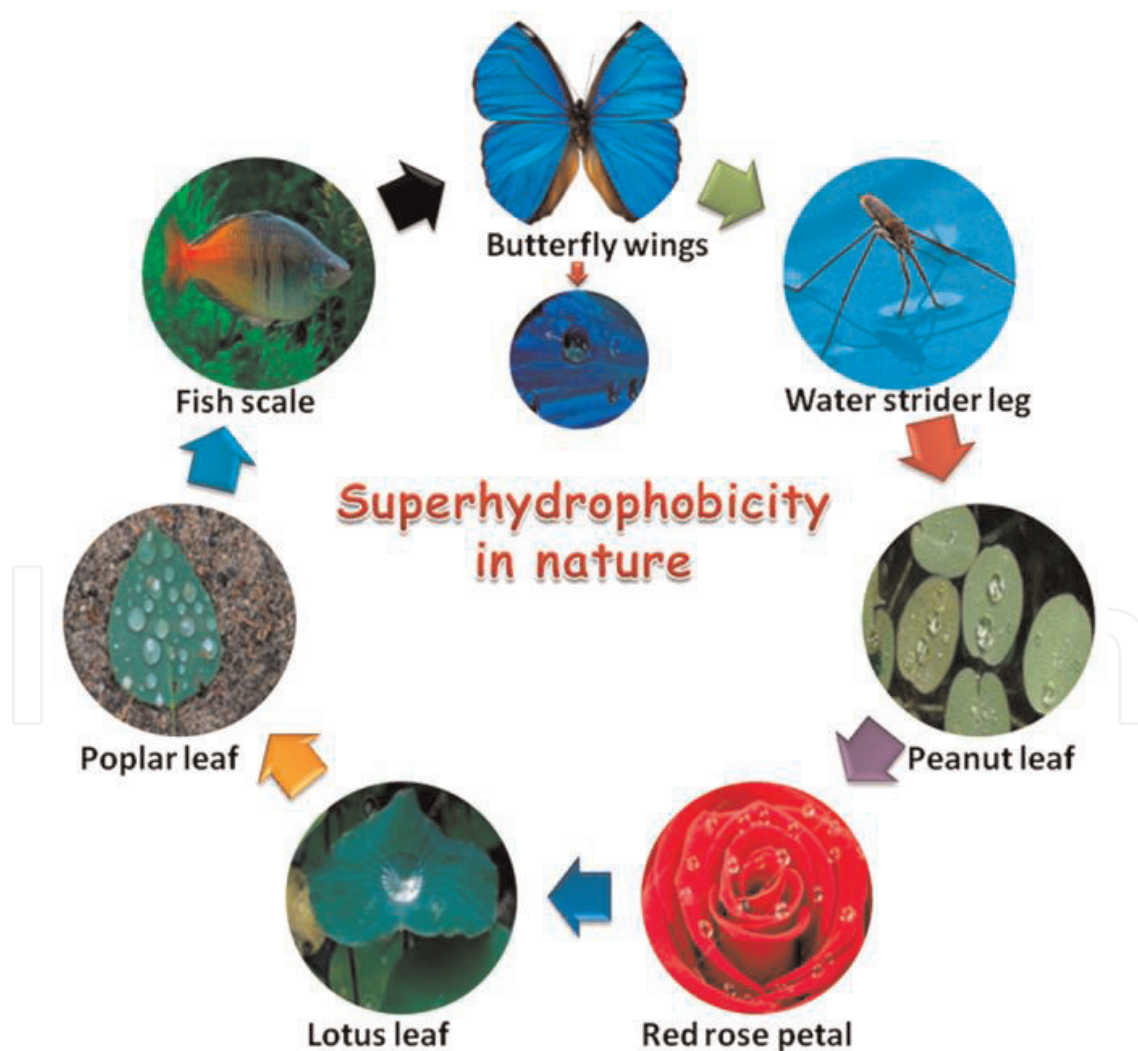


**Figure 1.** Superhydrophobicity in nature [3].

the surface. WCA is not the only parameter that is important to evaluate a superhydrophobic surface; other parameters like sliding angle and contact angle hysteresis are also important, which will show how slippery or sticky the surface is against a water droplet. These parameters will be discussed in depth later.

First, it is important to specify an ideal superhydrophobic coating. An ideal superhydrophobic coating has WCA higher than  $150^\circ$  (up to  $180^\circ$ , which is the theoretical limit), and also the sliding angle and contact angle hysteresis must be lower than  $10^\circ$  to guarantee low stickiness of the superhydrophobic surface against water.

This special wetting behavior will provide various special applications such as self-cleaning, anti-icing, antibacterial, oil-water separation, corrosion resistance, etc. for superhydrophobic surfaces and coatings.

## 1.2. Shortcoming and limitations

As mentioned before superhydrophobic surfaces and coatings have a special wetting behavior against water droplets which leads to various industrial applications. But one might ask: what hinders the application of these properties in industries?

Superhydrophobic coatings and surfaces are rather new due to their unique wetting behavior against water in comparison to other traditional coatings currently used in industries like powder and sol-gel coatings and other organic, inorganic, and metallic coatings. The traditional coatings do not possess high water contact angle and are usually hydrophilic, and more time is needed to improve quality and production costs of the superhydrophobic coatings.

The superhydrophobic coatings and surfaces must have two main features to achieve superhydrophobicity:

- a. Hierarchical micro- and nanoscale roughness on the surface
- b. Low surface energy

These two must be considered to fabricate a superhydrophobic surface. Various fabrication methods have been presented: These techniques are divided into two main categories including top-down and bottom-up. The top-down approach includes template-based techniques, lithography, and surface treatment by plasma. In the bottom to top approach, the structure is self-assembled and includes layer-by-layer deposition, chemical deposition, and colloidal assemblies. The methods to achieve superhydrophobicity are not limited to these methods, and there are several others like electrospinning, templating, chemical etching method, chemical vapor deposition, phase separation, electroless galvanic coating, sol-gel method, and thermal spray methods.

The main shortcoming of superhydrophobic coatings and surfaces is the low stability of the superhydrophobic properties or high cost of fabrication or lack of high-scale production capabilities. This leads to the limited use of superhydrophobic coatings. Although several promising approaches have been taken recently to increase mechanical stability, which will be discussed further in this chapter.

## 2. Surface wettability evaluation parameters

To investigate surface wettability, three main parameters are used. These three parameters are the water contact angle, contact angle hysteresis, and sliding angle. WCA is not enough alone to understand surface wetting behavior, and at least one (the CAH or SA) is needed to know how much water droplets stick to the surface. The definition of each parameter is provided below.

### 2.1. Water contact angle

Atoms and molecules of liquid and solid have higher energy on the surface because there are fewer chemical bonds on the surface. This energy is known as the surface tension or the surface free energy and shown by  $\gamma$  and is equal to energy per unit area needed to build surface in constant temperature and pressure ( $\text{J/m}^2$  or  $\text{N/m}$ ). In the case that solid and liquid are in direct contact with each other, the surface energy will be lower than in the situation in which these two are separated. The relation between surface energies and adhesion work is shown in the Dupre equation [14].

$$W_{SL} = \gamma_{SA} + \gamma_{LA} - \gamma_{SL}. \quad (1)$$

In this equation,  $W_{SL}$  is the adhesion work per unit area,  $\gamma_{SA}$  is the surface free energy between air and solid,  $\gamma_{LA}$  is the surface energy between air and liquid, and  $\gamma_{SL}$  is the surface free energy between liquid and solid.

When a water droplet is placed on the surface of the solid, these two will reach equilibrium, and the water droplet makes a specific angle with the surface known as water contact angle ( $\theta_0$ ). The below equation can calculate the total energy:

$$E_{\text{total}} = \gamma_{LA} (A_{LA} + A_{SL}) - W_{SL} A_{SL}. \quad (2)$$

In this equation,  $A_{LA}$  and  $A_{SL}$  are, respectively, liquid/air interface and liquid/solid interface. In this situation regardless of gravitational potential energy and in constant volume and pressure in the equilibrium,  $dE_{\text{total}}$  is considered equal to zero.

$$\gamma_{LA} (dA_{LA} + dA_{SL}) - W_{SL} dA_{SL} = 0. \quad (3)$$

For a droplet with constant volume,  $\theta_0$  can be calculated by the equation below:

$$dA_{LA}/dA_{SL} = \cos(\theta_0). \quad (4)$$

Then according to these equations,  $\cos \theta_0$  can be calculated by Young's equation.

$$\cos \theta_0 = (\gamma_{SA} - \gamma_{SL}) / \gamma_{LA} \quad (5)$$

## 2.2. Contact angle hysteresis

To define contact angle hysteresis, first advancing ( $\theta_a$ ) and receding ( $\theta_r$ ) contact angles must be introduced. Contact angle hysteresis is calculated by subtraction of advancing and receding contact angles.

$$CAH = |(\theta_a - \theta_r)| \quad (6)$$

Consider a water droplet on the surface; if water droplets withdrawn or somehow evaporated from the surface, at first the surface area between the water droplet and surface does not change, but after a while, it starts to recede from the surface with a constant water contact angle equal to  $\theta_r$ .

If at a controlled condition, the volume of water droplet increases by a syringe or is cooled down on the surface, at first, the volume increases without change in surface area in contact with the solid until it begins to advance on the surface with a constant water contact angle equal to  $\theta_a$ .

Both advancing and receding contact angles on a surface depend on surface chemistry and topography, and a metastable droplet can have a contact angle between these two values which indicates the importance of measuring both of these values to evaluate surface wetting behavior [4].

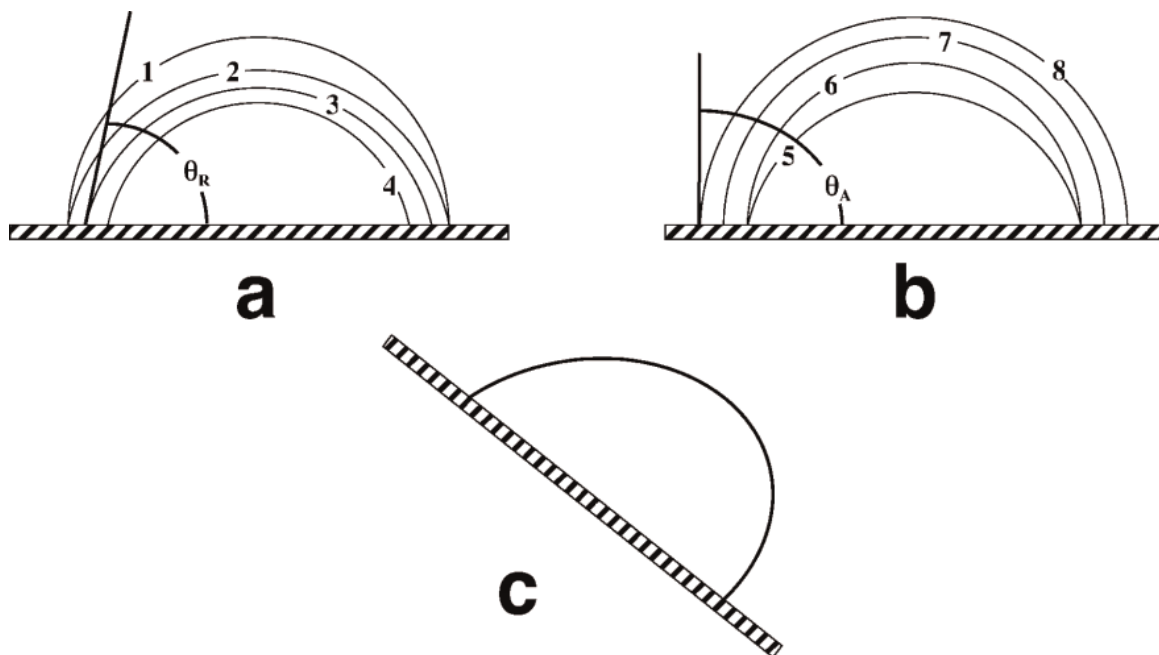


**Figure 2.** Schematics indicating the  $\theta_a$  and  $\theta_r$  (a and b, respectively) and a droplet on a tilted surface with  $\theta_a$  in front and  $\theta_r$  in the back [4].

Now consider a droplet on a tilted surface. While the droplet is moving downwards on a tilted surface, in the front, it expands, which will occur with a constant contact angle of  $\theta_a$ , and on the back, it shrinks with a constant contact angle of  $\theta_r$ , which is shown in **Figure 2c** [4].

### 2.3. Sliding angle

The sliding angle is another parameter to evaluate the wetting behavior of the surface in which a droplet with a certain weight is dropped onto the surface and the sliding angle is the critical angle that a droplet starts to move and slide downwards. Sliding angle and contact angle hysteresis are both used to evaluate adhesion of droplet to surface. Contact angle hysteresis is more detailed and difficult to measure than the sliding angle [5].

## 3. Wetting models

### 3.1. Young's model

Several wetting models have been defined to calculate contact angle on the surface. The first wetting model is Young's equation that was just mentioned. This model does not consider surface roughness of the solid surface. Below Young's equation is shown.

$$\cos\theta = \frac{\gamma_{SG} - \gamma_{SL}}{\gamma_{LG}} \quad (7)$$

In this equation  $\theta$  is the contact angle, and  $\gamma_{SG}$ ,  $\gamma_{SL}$ , and  $\gamma_{LG}$  are, respectively, the surface free energy of solid/gas, solid/liquid, and liquid/gas interface.

### 3.2. Wenzel model

It is obvious that in most cases the surface is not smooth, so Young's equation is not able to calculate the contact angle properly, so the Wenzel equation was introduced. In this equation, it is considered that the surface wetting occurs uniformly:

$$\cos\theta_w = r\cos\theta \quad (8)$$

In this equation  $\theta_w$  is the Wenzel contact angle,  $\theta$  is Young's contact angle, and  $r$  represents the surface roughness factor that is equal to ratio of real surface to apparent surface.

### 3.3. Cassie-Baxter model

As mentioned before wetting is considered to be uniform in Wenzel's equation, or in other words, it is considered that water went through all surface cavities and there is no dry part. On the other hand, there is another wetting model which considers that the wetting is not uniform and air packets do not let water get into the surface cavities. In this case, water is in contact with solid and air packets, and water contact angle with air is equal to  $180^\circ$ . The model is called Cassie-Baxter and the equation is shown below:

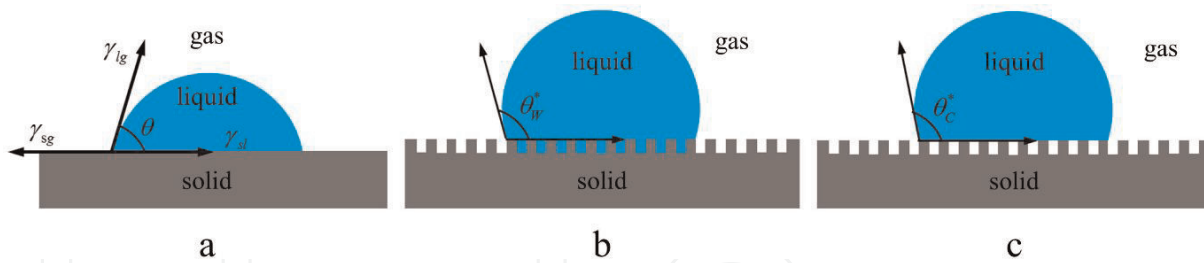


**Figure 3.** Schematics showing the difference between (a) young, (b) Wenzel, and (c) Cassie-Baxter wetting models.

$$\cos \theta_{CB} = f_1 * \cos \theta_1 + f_2 * \cos \theta_2 \quad (9)$$

$$\cos \theta_{CB} = f_1 * \cos \theta_0 + f_2 * \cos (\pi) \quad (10)$$

$$\cos \theta_{CB} = f_1 * \cos \theta - f_2 \quad (11)$$

$$\cos \theta_{CB} = f_1 * (\cos \theta + 1) - 1 \quad (12)$$

In the above equations,  $\theta_{CB}$  is the Cassie-Baxter contact angle,  $f_1$  is the ratio of the area that liquid is in contact with solid, and  $f_2$  is the ratio of the area that liquid is in contact with air packets made or trapped inside the surface cavities. In **Figure 3** the difference between the three aforementioned wetting models is shown.

### 3.4. Transition between wetting models

In case of a hydrophobic surface or coating surface wettability respects to one of Wenzel or Cassie-Baxter models. In an ideal condition, a superhydrophobic coating should be seen in the Cassie-Baxter model. In the Cassie-Baxter model as mentioned before the topography and surface energy is in a way that droplet cannot penetrate through the empty space between micro- and nanoscale pillars on the surface while in Wenzel model the surface structure is large enough for water droplets to penetrate. Droplet adhesion to surface is more considerable in the Wenzel model than in the Cassie-Baxter model due to penetration of droplet into the micro- and nanoscale grooves on the surface.

Change in surface roughness and energy will lead to a transition from the Wenzel to the Cassie-Baxter model, which depends on the hierarchical micro- and nanoscale roughness on the surface. An easy way to evaluate whether the transition between Wenzel and Cassie-Baxter model has occurred or not is to measure the sliding angle. A noticeable decrease in sliding angle will be observed after the transition from the Wenzel to the Cassie-Baxter model due to increase in surface roughness and fabrication of hierarchical micro- and nanoscale roughness.

## 4. Applications of superhydrophobicity

Superhydrophobic surfaces and coatings as mentioned have a unique behavior against water droplets. This unique behavior results in a new set of applications including self-cleaning, anti-icing, antibacterial, oil-water separation, corrosion resistance, etc.

#### 4.1. Oil-water separation

There have been many reports of oil contaminations in sea waters and rivers due to leak of factory waste into nature and accidents like Deep Water Horizon and Sanchi oil tanker collision. Removing oil contaminations from the water was always challenging and expensive, so different methods have been introduced by scientists to remove the oil contaminations. These methods are categorized into three main groups including water removal, oil removal, and smart controllable separators [6]. The water removing filters are superhydrophilic and superoleophobic; this kind of filter works underwater, and when they get wet by water, the presence of the water on the surface of the filter prevents oil to pass from the filter pores. The category in the oil removing method is a more efficient way because the amount of oil is always less than the amount of water, so it is logical that we try to remove the oil from water and not water from oil. To remove oil from water, the material should be superhydrophobic and superoleophilic; this mostly depends on the surface energy. The surface energy should be lower than the water surface tension ( $72.8 \text{ mN m}^{-1}$ ) and higher than the oil surface tension

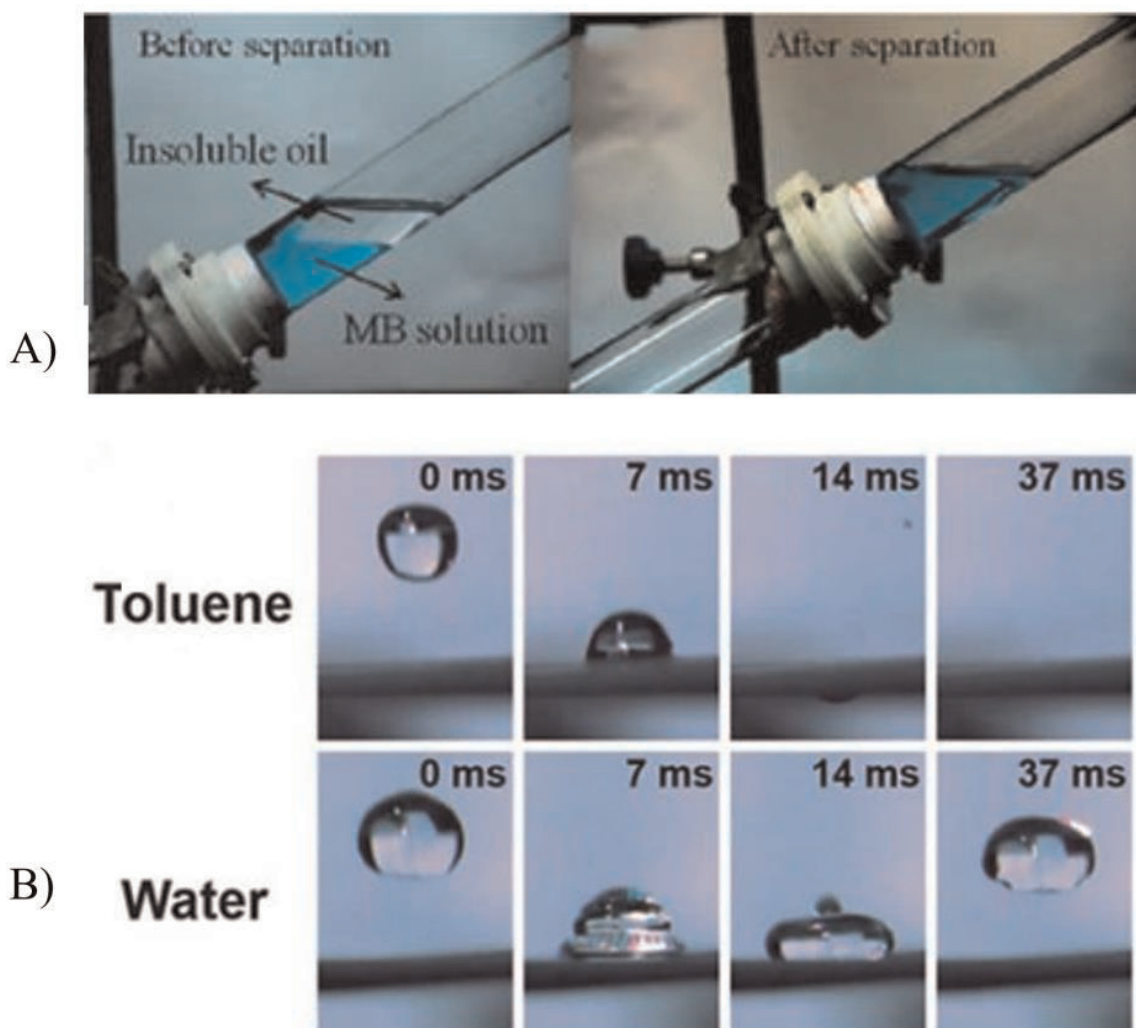


**Figure 4.** (A) Oil-water separation with the use of  $\text{TiO}_2$ -coated superhydrophobic and superoleophilic mesh, (B) opposite behavior of silicone elastomer-coated mesh against water and toluene droplets [7].

( $30 \text{ mN m}^{-1}$ ). The oil removing method has two subcategories including oil removing filters and oil absorbents (like oil absorbent sponges, etc.)

Superhydrophobic oil removing filters are the main part of the oil removing category. Feng et al. [7] used a  $\text{TiO}_2$ -coated mesh to separate oil from water (see **Figure 4a**). Parkin et al. [8] used a silicone elastomer coating on a mesh to efficiently separate organic solvents like hexane, petroleum ether, and toluene from water. As shown in **Figure 4b**, the water droplet cannot pass through the filter, but toluene can easily pass through.

Also, absorbent materials are considered as a part of this group that can collect oil and changes it from liquid to a semi-solid phase. Tai et al. [9] built a graphene base sponge with high sensitivity and suitable recyclability (**Figure 5a**). The sponge was able to absorb oil up to 165 times of its weight. Pan et al. [10] built a three-dimensional superhydrophobic material through a one-step immersion process. This material had a high oil absorption capacity and was able to separate oil from water efficiently (**Figure 5b**). Superhydrophobic sponges could be used up to 300 times without losing their properties in an ideal situation. Currently, there are several serious challenges in this field. One of the main problems is the instability of the hierarchical structure of the coating on sponges that could easily get damaged by mechanical stresses or by exposure to chemical pollutions (acids, etc.). Also, most of the studies in this field worked on separation of oils with low density, and very few studies have been done on high-density oils [6].

#### 4.2. Corrosion resistance

There are several ways to protect a surface from corrosion. One of the ways is to use different coatings or to use some processes to add heavy materials like chrome onto the surface which is harmful to the environment [11]. During the past two decades, scientists have been using superhydrophobic nanocomposite coatings without any toxic materials to protect various surfaces from corrosion [12–14]. The corrosion protection capability of the superhydrophobic coatings mainly is because of the presence of air pockets between surface and corrosive

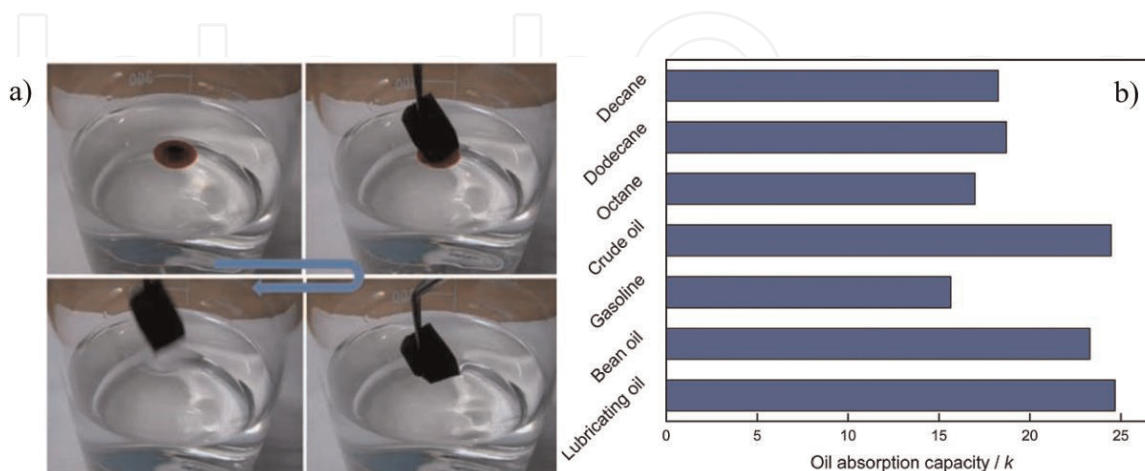


**Figure 5.** (a) Engine oil removing process using a superhydrophobic sponge [9], (b) the absorption capacity of superhydrophobic sponges for different nonpolar oil and solvents [10].

solution, and these packets act like a barrier and prevent corrosive ion diffusion and protect the substrate [15].

Advincula et al. [16] built a superhydrophobic corrosion-resistant nanostructure coating by using a conductive polymer in a two-step process. This coating could be deposited on any metal surface. They studied the corrosion resistance of the nanocomposite coating by the use of polarization test in NaCl solution in different pH and temperatures for 7 days, and the corrosion protection efficiency was reported to be higher than 95%.

Zhang et al. [17] worked on superhydrophobic membranes with different morphologies and chemical compositions through the sol-gel method. Humid air test and polarization tests showed insufficient corrosion protection. They realized that surface morphology is more important than the chemical composition of the sol-gel coating. In another study on the corrosion resistance of coatings on the Mg-Mn-Se alloy, three types of coatings with different wettabilities from hydrophilic to superhydrophobic were deposited on substrates, and corrosion resistance of the coatings in 3% NaCl solutions was studied [18]. Corrosion potential is known to be a criterion for corrosion resistance; the higher potential shows higher corrosion

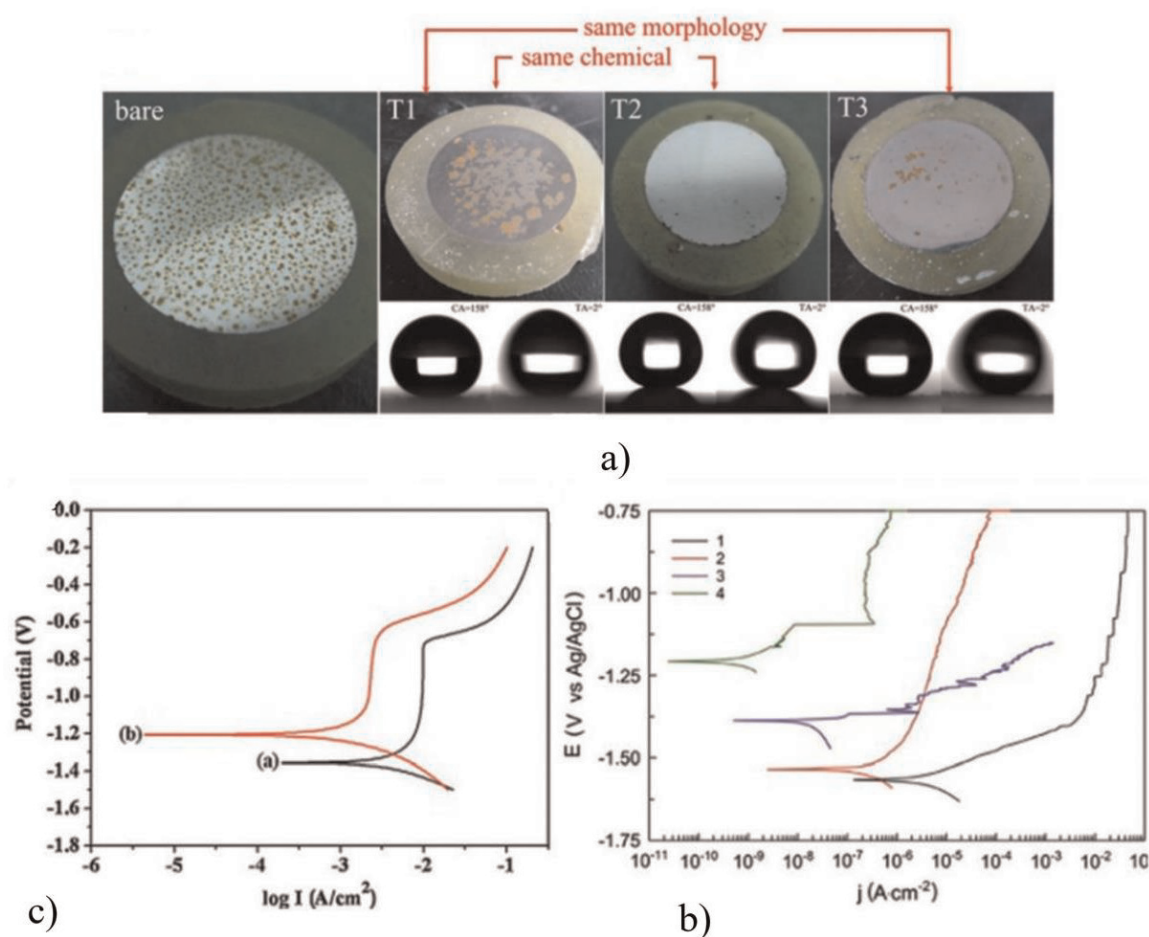


**Figure 6.** (a) Coating with different wettability after humid air test [17]; (b) polarization curve of the samples in 3.5%wt NaCl solution: (1) alloy without coating, (2) coated sample with PEO method, (3) hydrophobic coating, and (4) superhydrophobic nanocomposite coating [18]; and (c) polarization curve of the superhydrophilic Al (black line) and superhydrophobic PU/Al/Al<sub>2</sub>O<sub>3</sub> in NaCl solution [20].

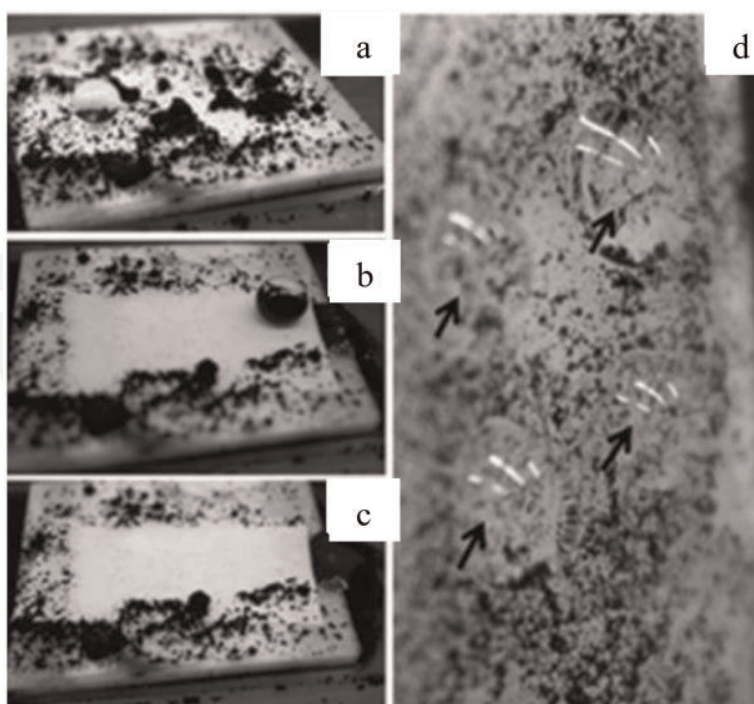


**Figure 7.** (a, b, c) Showing self-cleaning properties of the superhydrophobic high-density PE with  $\text{TiO}_2$  nanoparticles; (d) adhesion of water droplet to high-density PE coating while the sample is held vertically [24].

resistance in general [19]. Superhydrophobic nanocomposite coating deposited with plasma electrolytic oxidation<sup>1</sup> on Mg alloy showed the best results in polarization tests (**Figure 6b**). Li et al. [20] managed to build a superhydrophobic corrosion-resistant polyurethane coating containing  $\text{Al}_2\text{O}_3$  nanoparticles. The water contact angle of the coating with 2 wt% PU was  $151^\circ$ , and the sliding angle was  $6.5^\circ$ . An increase in corrosion potential showed the positive effect of superhydrophobic coating in corrosion protection (**Figure 6c**).

### 4.3. Self-cleaning properties

The lotus leaf's surface is always clean regardless of any contamination that may be present in its surrounding environment [21]. This leaf has a unique surface structure and is coated with wax and shows superhydrophobic properties, and the sliding angle is very low so water can easily slide on the surface of the leaf and remove any contamination. The aforementioned properties of superhydrophobic surfaces and coatings are called self-cleaning properties. Many superhydrophobic coatings were synthesized with different methods and used in industries, daily, or in military use [22, 23].

Lions et al. [24] produced a nanocomposite self-cleaning superhydrophobic high-density PE coating containing  $\text{TiO}_2$  nanoparticles. Results showed that water droplets could remove big alumina particles or small graphite particles from the surface of the coating (**Figure 7a-c**). On the other hand, high-density PE by itself had a smooth surface which resulted in water

<sup>1</sup>REO.

droplets sticking on the surface of the coating, and the coating could not have self-cleaning properties (**Figure 7d**). Rodriguez et al. [24] also managed to build a coating based on lotus leaf surface morphology. This coating was made by nanostructure template assembly, and the sliding angle was between  $4^\circ$  and  $7^\circ$ . The self-cleaning properties of this coating were very close to that of a lotus leaf.

But the question is how a superhydrophobic surface has self-cleaning properties. The first reason is due to surface energy calculations. To explain how even hydrophobic particles can be collected by rolling drop will be further discussed.

When a spherical particle (pollution) is in contact with water on the sample surface (**Figure 8**), the area of the wetted surface can be calculated by the equation below in which  $2R_s$  is the sphere diameter:

Area of the wetted part of the particle on the surface (pollution) =  $2\pi R_s^2(1 + \cos \theta_e)$

Also, the liquid will lose some of the area of itself that can be calculated through the below equation:

Lost area of the liquid =  $\pi R_s^2 * \sin \theta_e$

The change in surface energy can be calculated by the below equation:

$$\Delta F = 2*\pi*R_s^2*(1 + \cos\theta_e)(\gamma_{sl} - \gamma_{sv}) - \pi R_s^2 - \sin\theta_e*\gamma LV \quad (13)$$

$$\Delta F = \gamma LV * 2*\pi*R_s^2*(1 + \cos\theta_e)^2 \quad (14)$$

When the equivalent water contact angle is not  $0^\circ$  and  $180^\circ$ , the particle always tends to attach to a spherical-shaped water droplet. The second reason for self-cleaning of these rough surfaces is that the contact area between the pollution particle and solid surface is very limited due to the unique surface roughness so the pollution particle has a very lower adhesion to the surface in comparison with smooth surface also water can diffuse into larger porosities as a result of impacting to the surface. The diffused water will absorb particles and get back to the top of the surface due to superhydrophobic properties and lead to self-cleaning properties [25].

Chen et al. [26] introduced a unique mechanism for self-cleaning surfaces by inspiration from Cicada wings (**Figure 9**). On this surface, pollutions are automatically removed due to the bouncing movement of water droplets on the surface. The ability of the pollutant particle to



**Figure 8.** Schematic of the spherical particle that has moved from air into the water; the contact angle between the particle and water is shown [25].

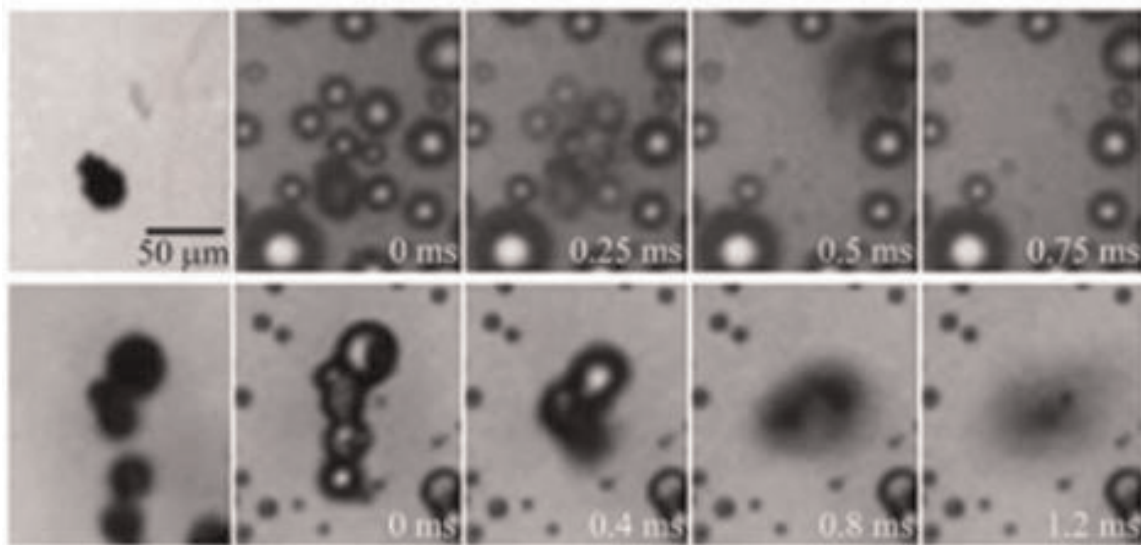


**Figure 9.** Self-cleaning properties of coating inspired from Cicada wing through bouncing movement of the pollutant particle on the surface [26].

bounce on the surface of the superhydrophobic coating mostly depends on the stability of the particle into the liquid phase. This unique coating shows there is a chance to produce and develop new self-cleaning coatings.

#### 4.4. Anti-icing properties

Every year ice storms harm the electrical transmission equipment, communication systems, highways, etc. [27]. To reduce these kinds of damages, different methods of producing an anti-icing surface have been introduced [28]. Although there are other conventional methods like reducing icing temperature point and thermos electrical and mechanical methods, these methods use a lot of energy and are not economical.

In recent years superhydrophobic coatings have been suggested as an anti-icing coating. As mentioned before, the presence of air pockets on the superhydrophobic nanocomposite coating structure causes the water droplets to slide easily on the surface; therefore there will not be enough time for the droplet to frost on the surface [29–31]. In situations that the temperature is very low, superhydrophobic nanocomposite coatings can be used to prevent water from wetting the surface and cause frost and finally damage to the surface or equipment [32]. Chen et al. [33] deposited four types of coatings with different wettabilities from superhydrophilic to superhydrophobic on Al substrate. Dynamic studies of droplet impact to the superhydrophobic surface at low temperature showed that if the angle between the direction of droplet and surface of the coating is higher than  $30^\circ$ , then water droplet can easily slide and be removed from the surface. Hen et al. [34] produced a superhydrophobic nanocomposite film containing multi-walled silicon nanotubes. Results showed that the growing rate of ice on the non-coated Al surface is twice the surface with superhydrophobic nanocomposite coating (**Figure 10**).

In another study, an easy and low-cost nanocomposite coating containing polydimethylsiloxane with different coupling agents was investigated [35]. As shown in **Figure 11**, the superhydrophobic coating is completely effective in reducing ice adhesion to the surface up to 97%.

Scientists have some disagreements about the relations between superhydrophobicity and anti-icing properties. Some believe that these two are not related to each other; on the other hand, some insist that superhydrophobicity will result in anti-icing properties [36]. These disagreements are because there is no specific standard that can be used to evaluate ice adhesion to surfaces; also the method of preparing ice for each study is different from the

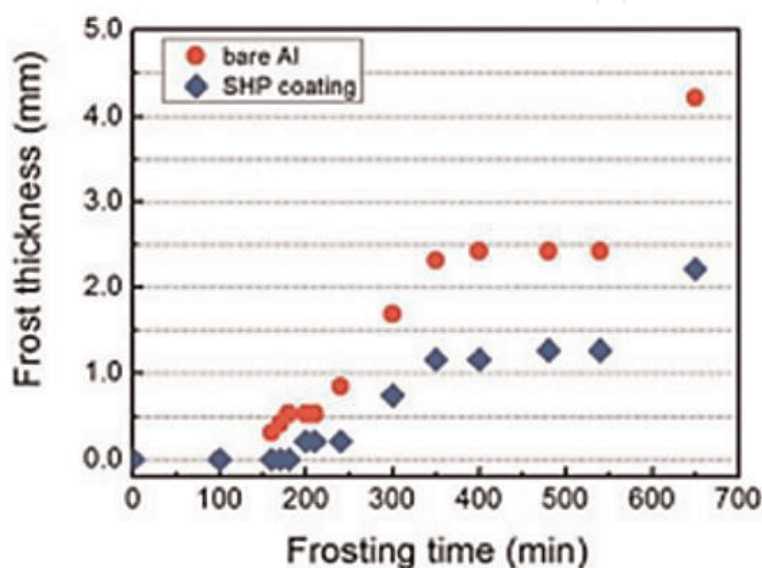


**Figure 10.** Comparison of ice growing rate on bare Al and Al with superhydrophobic nanocomposite coating containing multi-walled silicon nanotubes [34].



**Figure 11.** Comparison of the uncoated and superhydrophobic coated sample at  $-5^{\circ}\text{C}$  and high humidity [35].

other, so by now it is not possible to have a definite answer to this matter [28]. The recent studies have helped to get a better understanding of the ice formation process on the superhydrophobic surface, but there is still much left unknown about the nucleation, growth, and adhesion to the surface which need more studies and information on this subject.

#### 4.5. Drag reduction

One of the main problems that a solid moving in water like a submarine is facing is the drag force; this force has resulted from the friction force between water and solid surface which is moving through water. There are several examples in nature which show antidrag properties [37]. By inspiration from shark skin and lotus leaf, several superhydrophobic coatings were fabricated [38]. Here, the positive effect of superhydrophobicity on drag reduction will be discussed. As mentioned before superhydrophobic coatings have some air pockets inside their hierarchical micro- and nanoscale surface structure which will reduce the contact between solid and liquid so the drag force will dramatically reduce [39]. Drag reduction phenomenon by superhydrophobic surfaces was first reported in 1991 [40]. Muan et al. [41] studied the effect of superhydrophobic nanocomposite coating on drag reduction in linear and turbulent streams. This superhydrophobic coating contained  $\text{TiO}_2$  nanoparticles and was deposited on

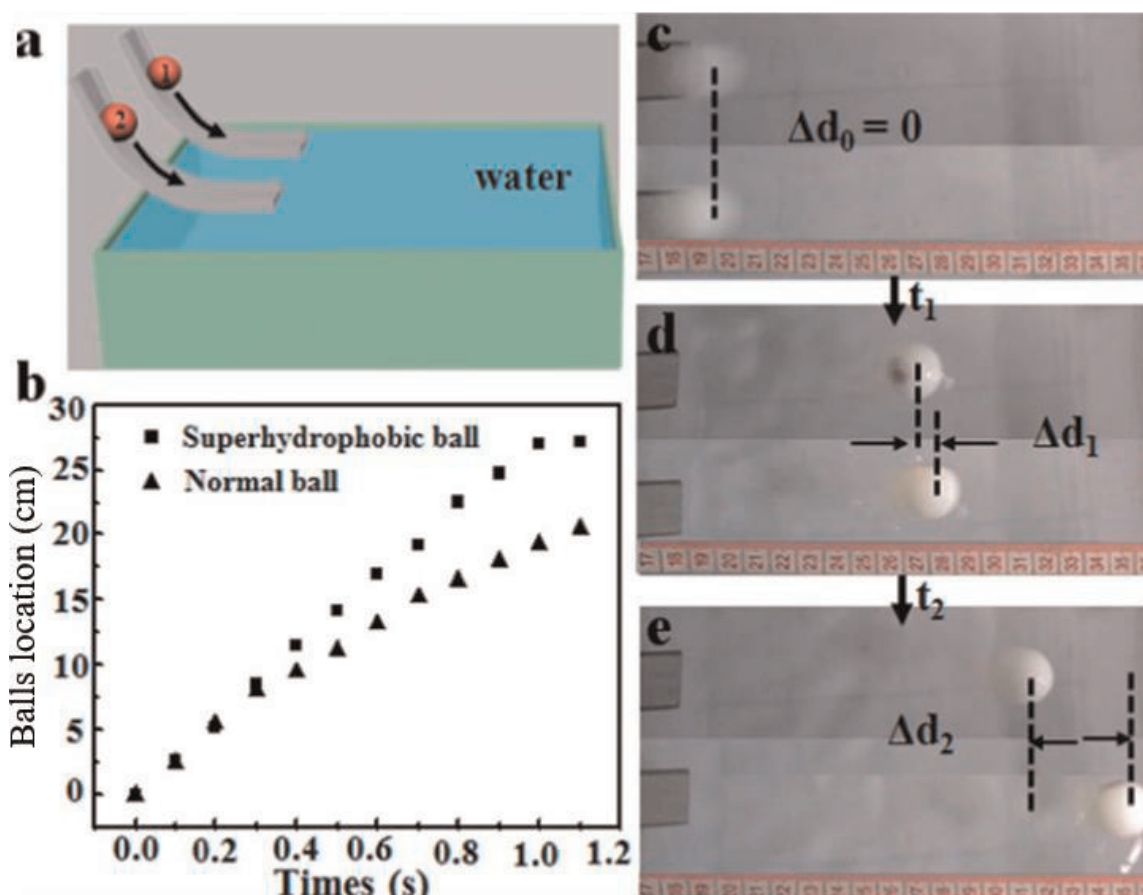


**Figure 12.** (a) Schematic of set up to throw balls into the water in the same condition, (b) balls' location-time diagram, (c, d, e) balls' picture at  $t_1 = 0$  s,  $t_2 = 0.61$  s, and  $t_3 = 1.11$  s [42].

the Al substrate, and the drag force on this sample was compared with non-coated sample. Results showed that superhydrophobic coating will reduce drag force up to 30% for linear and 15% for a turbulent stream. Chen et al. [42] coated a ball with superhydrophobic coating; then they used a stage as shown in **Figure 12** to throw a ball with superhydrophobic coating and one without any coating; the ball with superhydrophobic coating had an average speed of  $27.0 \text{ cm min}^{-1}$ , but the average speed of ball without coating on water was  $12.5 \text{ cm min}^{-1}$ . This indicates that the superhydrophobicity is completely effective in the reduction of drag force and facilitates moving through water. On the other hand, Wei et al. [43] had a different opinion about this phenomenon. They believed that drag reduction is not because of the lower solid and liquid contact and the plastron effect is the main reason of this phenomenon. They fabricated a superhydrophobic coating by electrodeposition of gold on substrate. This superhydrophobic coating reduced the drag force up to 38.5% in speed of  $0.46 \text{ m s}^{-1}$  which is amazing. They said that reduction in water contact angle of the superhydrophobic coating will have a very small effect on drag reduction and will change it into 32.7%. They concluded that the main reason for drag reduction is not the high water contact angle but it is because of the plastron effect [44]. On a non-coated sample, the friction is just between solid and water, but on a superhydrophobic surface, there are three phases, water, solid, and trapped air between these two, so the friction will be drastically reduced in this situation that is known as the plastron effect.

#### 4.6. Antibacterial properties

Antibacterial properties are essential in biosensors, implants, food packaging, and industrial and marine equipment [45, 46]. For example, one of the main reasons that cause infection in patients after surgery is bacteria that grow on implants [46]. To solve this problem, antibacterial coatings that reduce the bacterial adhesion to the surface or coatings containing antibacterial additives are suitable [47]. Schoenfisch et al. [47] produced a zero gel with the ability of nitrogen oxide release by spray method. In this case a combination of superhydrophobicity and nitrogen oxide release will result in a very strong antibacterial property. Nitrogen oxide showed a positive effect after some time and reduced the number of alive bacteria that had attached to the superhydrophobic surface. Ivanova and Philipchenko introduced an easy method to produce superhydrophobic coating by using chitosan nanoparticles. Antibacterial property is enhanced because of chitosan nanoparticles. Usage of nanosilver particles in superhydrophobic coatings also enhances the antibacterial properties; this enhancement is due to diffusion into the bacterial cell and damages the DNA structure from the inside [48]. There are still some doubts and questions about the mechanism of silver antibacterial properties. Heinonen et al. [49] fabricated a superhydrophobic coating containing silver nanoparticles through the sol-gel method. First silver nanoparticles were attached to  $\gamma$ -alumina by the Tollens process, and then the composite coating was functionalized with fluoroalkyl silane<sup>2</sup> to reduce the surface energy. The diagram in **Figure 13** shows the number of bacteria on non-coated steel, superhydrophobic coated steel, and superhydrophobic coating

---

<sup>2</sup>FAS.

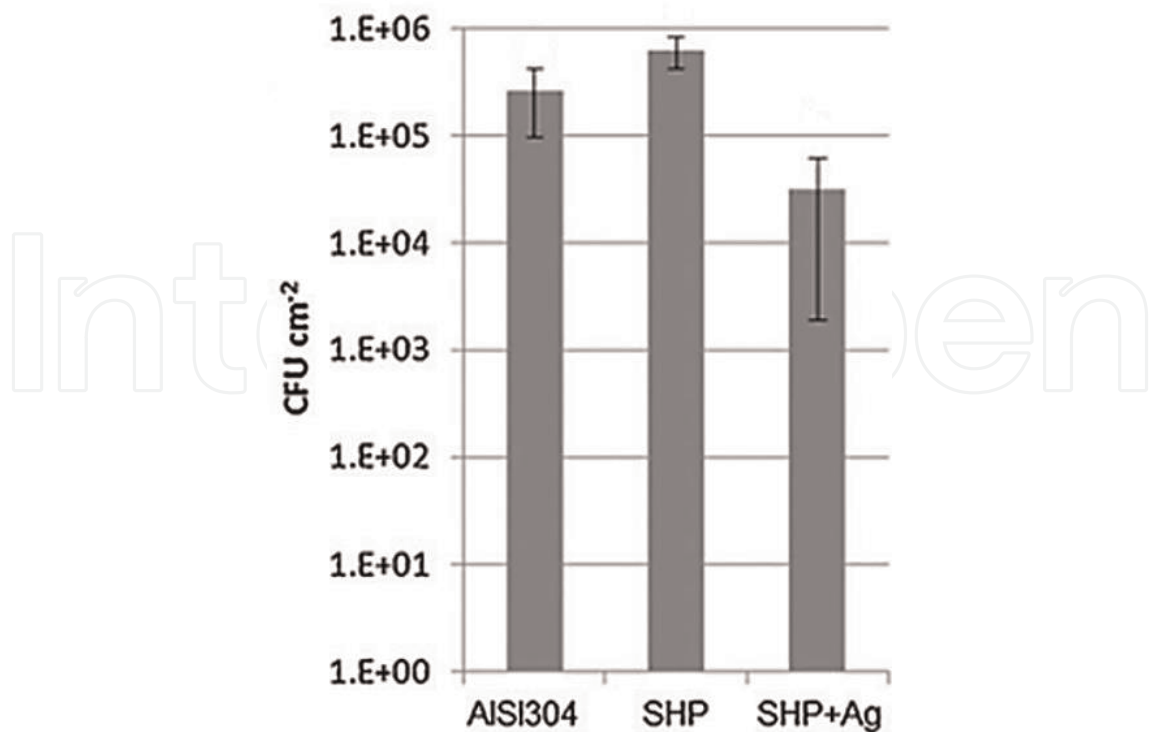


**Figure 13.** It shows the number of bacteria on non-coated steel (AISI304), superhydrophobic coated steel (SHP), and superhydrophobic coating with nanosilver particles steel (SHP + Ag) after 1-day exposure to bacteria at 25°C [49].

with nanosilver particle steel after 1-day exposure to bacteria at 25°C; the superhydrophobic coating with silver nanoparticles reduced the alive bacteria on the surface up to 88%.

Xue et al. [50] used the same method to fabricate silver nanoparticles on cotton fibers. After that hexadecyltrimethoxysilane was used to modify these fibers, and superhydrophobicity was achieved. As shown in **Figure 14**, non-coated cotton fiber does not have any resistance

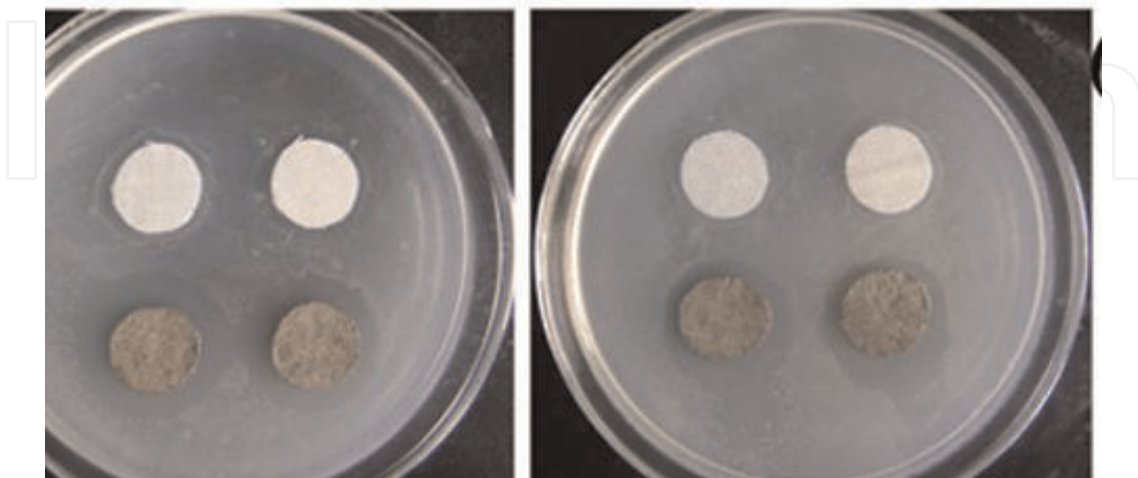


**Figure 14.** Comparison of antibacterial properties on non-coated cotton fiber (the white ones) and superhydrophobic coated fiber cottons (the gray ones) [50].

against bacteria, but on the other hand, the superhydrophobic coated sample with nanosilver additives destroys almost all of the bacteria from its surface.

In general, superhydrophobic coatings are not an ideal antibacterial coating, and in some cases, instability, toxicity and low durability of these coatings make them a problematic method for antibacterial purposes. So, further studies in this field are needed to overcome the current problems.

## 5. Fabrication methods

Several techniques have been introduced to fabricate superhydrophobic surfaces. These techniques are divided into two main categories including top-down and bottom-up. The top-down approach includes template-based techniques, lithography, and surface treatment by plasma. In the bottom to top approach, the structure is self-assembled and includes layer-by-layer deposition, chemical deposition, and colloidal assemblies. The methods to achieve superhydrophobicity are not limited to these methods, and there are several others like electrospinning, templating, chemical etching method, chemical vapor deposition, phase separation, electroless galvanic coating, sol-gel method, and thermal spray methods.

### 5.1. Wet chemical

#### 5.1.1. Chemical etching method

Chemical etching and other methods like plasma etching can be used to introduce micro- and nanoscale roughness to the substrate. Also, this process can be combined with other methods of fabrication superhydrophobic coatings to improve special surface roughness that is needed. Almost in all studies, chemical etching and similar methods like that are followed by surface modification with low surface energy materials like fatty acids, fluoroalkyl silanes, etc. This kind of superhydrophobic surfaces only has laboratory usage. Because of their low stability, they are mainly used to study the behavior of superhydrophobic surfaces against water in different situations, but the combination of this method with others seems promising.

Song et al. [51] used  $\text{CuCl}_2$  solution to do chemical substitution reaction on Al substrate to make hierarchical micro- and nanoscale roughness on the Al substrate which is necessary to achieve superhydrophobicity. After the chemical etching, the surface was modified with a fluoroalkyl silane solution to increase the WCA to higher than  $150^\circ$ . In this study, 1 molar  $\text{CuCl}_2$  solution was used and different etching times were tried. Also, the effect of removing the deposited Cu on substrate was investigated. As mentioned before this method is a chemical substitution reaction and a Cu element deposit on the Al surface while  $\text{Al}^{3+}$  gets into solution; the deposited Cu on the surface does not have a chemical bond with the surface and can be removed by an ultrasonic bath in water. So, to study the effect of Cu removal from the substrate, samples were washed in an ultrasonic bath. After the chemical etching, all samples were put into a fluoroalkyl silane solution.

When the aluminum plate is immersed into the  $\text{CuCl}_2$  solution, the chemical substitution starts, and copper ions react with the aluminum element on the surface, and aluminum chloride will be made by this reaction. As a result, the copper element will deposit on the

surface. The aluminum corrosion potential is lower than copper, so when copper deposits on the surface of the aluminum, a galvanic reaction will occur, and reaction speed will be increased. This reaction is exothermic and produces a lot of heat. In addition to this, the copper on the surface reacts with solution water, and hydrogen ions will be produced which will make the solution acidic and be able to remove aluminum from the substrate. When the

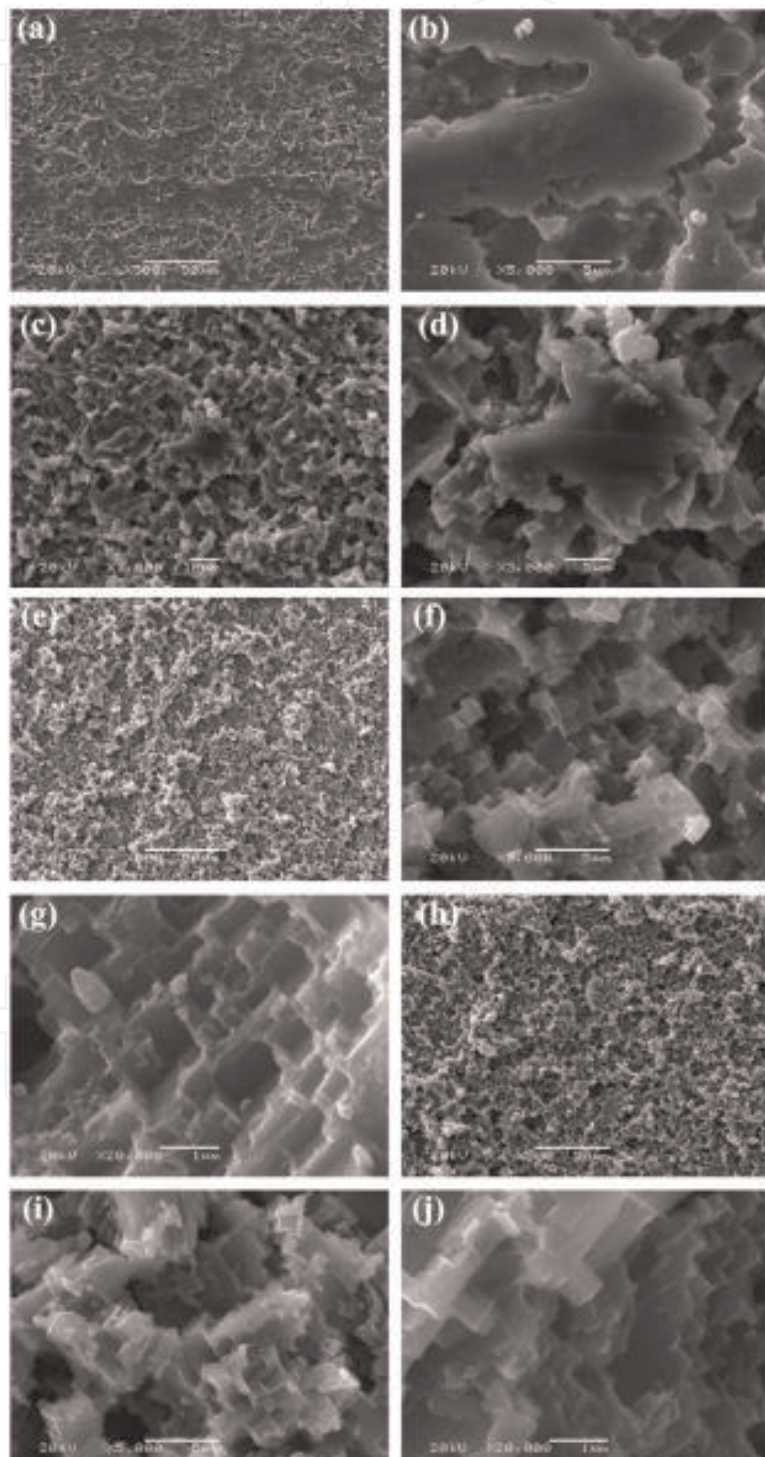


**Figure 15.** SEM image of etched aluminum surface in  $\text{CuCl}_2$  solution in different periods of time: (a, b) 1 s, (c, d) 3 s, (e, f, g) 10 s, (h, i, j) 70 s [51].

hydrogen ions react with the aluminum on the surface of the sample, then a small hydrogen bubble will be made on the surface so during that time the copper ions cannot affect that part of the sample. As a result, the corrosion will not be uniform. This will be beneficial to achieve hierarchical micro- and nanoscale roughness. Below the reactions are mentioned.



The aluminum plate is a polycrystalline metal that has grain boundaries and dislocations; these places are ideal for corrosion and chemical substitution, so immediately after immersion of Al plate into the  $\text{CuCl}_2$  solution, the reaction will take place in these places. As a result, rectangular planes and nanoscale steps will be formed on the surface. In **Figure 15**, SEM image of the surface after chemical etching for different periods is shown. It is worth mentioning that the samples were washed in water by ultrasonic bath [51].

- Efficient conditions to make a hierarchical structure on the Al substrate through chemical etching

In the aforementioned study, the effect of removal of deposited copper on the substrate was studied. In the results as can be seen in **Figure 16** in which the copper had been removed from the surface through ultrasonic bath, the stability of the superhydrophobicity is higher [51].

- Crucial role of surface modification after the chemical etching process

Chemical modification and reducing surface energy are necessary to achieve superhydrophobicity. Surface modification of the smooth surface with fluoroalkyl silane will increase the

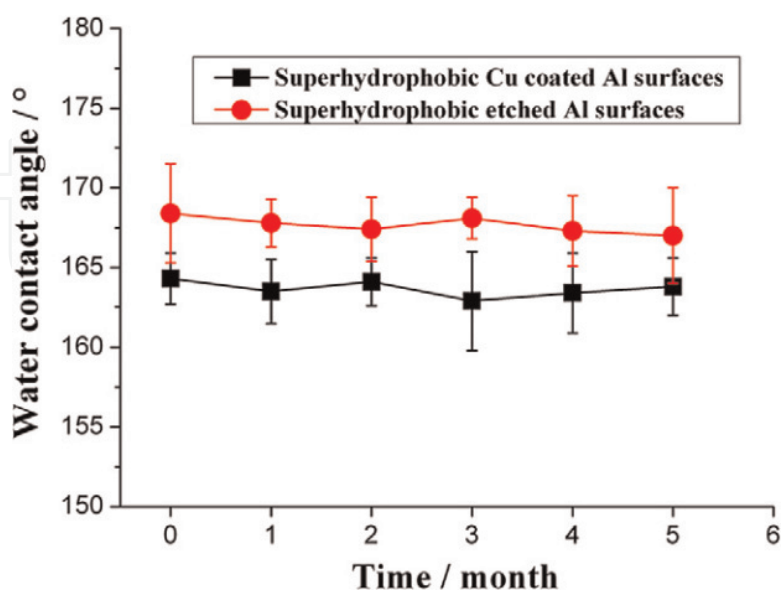


**Figure 16.** WCA measurement of the superhydrophobic samples during time (black line (with deposited copper), red line (without the deposited copper)) [51].

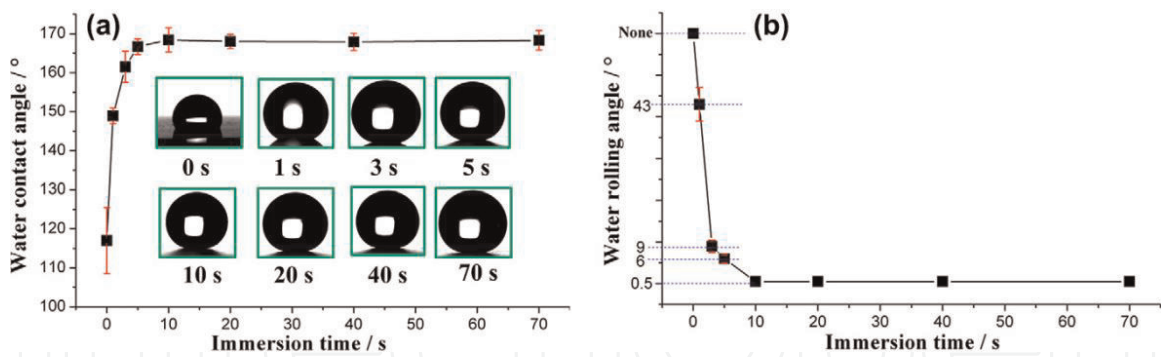


**Figure 17.** Change in WCA for different times of etching process (all samples were chemically modified with fluoroalkyl silane solution) [51].

WCA up to 117 which indicates the effect of surface energy. **Figure 17** shows WCA measurement results for samples with a different etching time which were chemically modified with fluoroalkyl silane solution before WCA measurements. As can be seen for etching time higher than 10 seconds, an enormous improvement in hydrophobicity is shown, and the superhydrophobicity was achieved. The reason for this improvement is the combination of hierarchical micro- and nanoscale roughness caused by chemical etching followed by low surface energy due to chemical modification with fluoroalkyl silane solution [51].

### 5.1.2. Sol-gel method

This method has been used in various studies to fabricate superhydrophobic coatings on different substrates. The sol-gel coating can be applied on the surface by various methods like dip coating, spin coating, spraying, etc. To achieve superhydrophobicity, the sol-gel coating is modified with a low surface energy material. Different approaches were taken to build a superhydrophobic coating, and some of them are mentioned here. After that, a more detail study about the sol-gel process will be provided.

One of the sol-gel coatings is alumina sol in which the aluminum tri-sec-butoxide was used as a precursor, and the particle size in sol was about 80 nm. The sol was deposited on the glass substrate by spin coating and cured at 400°C. The presence of nanoalumina particles in coating makes peaks on the surface of the coating with a height of 1 μm; and to achieve nano roughness, samples were put into boiling water for 5 minutes. As a result, a flower-like morphology was made on the coating, and after surface modification with low energy material, superhydrophobicity was achieved (look at **Figure 18a**) [52].

Mahadik et al. [53] used methyltrimethoxysilane as a precursor and fabricated a coating by the sol-gel method. The coating was deposited on the glass slides by dip coating and then cured at 150°C. After surface modification with trimethylchlorosilane, superhydrophobic properties were achieved. Coating WCA was 170 and it was stable up to 550°C but at temperatures higher than 600°C and after 2 h of exposure in this condition, the sample showed superhydrophilic properties which indicates that the surface chemical modification was destroyed. The superhydrophobicity was restored after doing the surface chemical modification with trimethylchlorosilane.

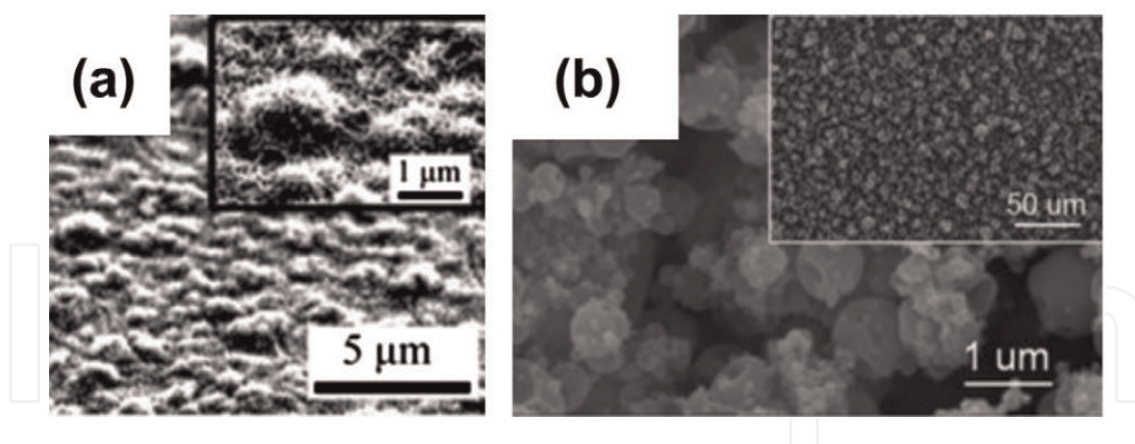


**Figure 18.** (a) SEM image of nanoalumina coating surface after 5-minute immersion into boiling water, (b) FESEM image of modified SiO<sub>2</sub> coating, which was deposited by electro spray method [53, 54].

Kim et al. [54] fabricated a superhydrophobic silica coating by electro spraying of sol-gel solution on the substrate. Tetraethoxysilane and methyltriacetoxysilane were used as sol-gel precursors. To achieve superhydrophobicity and self-cleaning properties, the coating was modified by perfluoro-octyl silane (**Figure 18b**).

Various studies have been reported in which sol-gel method was used to fabricate a rough surface and the low surface energy materials were used to reduce the surface energy and reach superhydrophobic properties, but almost all of the coatings suffered from lack of superhydrophobic property stability [55].

Superhydrophobic properties have been achieved on aluminum and silicon substrates by first fabrication of a rough surface on the substrate by either chemical bath deposition or electrochemical deposition or chemical etching, and then low surface energy treatments were done by FAS-17, stearic acid, or rf-sputtering of PTFE films [56–61].

Brassard et al. fabricated a superhydrophobic coating using the sol-gel method. They used the Stober process to fabricate SiO<sub>2</sub> nanoparticles from TEOS precursor, and then the synthesized nanoparticles were functionalized by fluoroalkyl silane. The functionalized SiO<sub>2</sub> nanoparticles were spin-coated in Al6061 substrate and dried at 70°C. The FTIR spectra results related to the functionalized SiO<sub>2</sub> nanoparticles are shown in **Figure 19**. The peaks 610 cm<sup>-1</sup>, 730 cm<sup>-1</sup>, 960 cm<sup>-1</sup>, 1000 cm<sup>-1</sup>, and 1250 cm<sup>-1</sup> are related to C—F bonds in CF, CF<sub>2</sub>, or CF<sub>3</sub> [62–65]. Also, the peaks at 1145 cm<sup>-1</sup> approve chemical bonding between SiO<sub>2</sub> particles and fluoroalkyl silane. The peaks at 430 cm<sup>-1</sup>, 800 cm<sup>-1</sup>, and 1100 cm<sup>-1</sup> are related to Si—O—Si bond.

The main problem with almost all the aforementioned superhydrophobic coatings is their lack of mechanical properties due to low adhesion and cohesion of the coatings. The articles about these kinds of superhydrophobic coatings do not consider the mechanical properties and stability, and they just focus on the effect of other coating parameters on the WCA of the coating. Khodaei and Shadmani [66] fabricated a superhydrophobic nanocomposite coating using the sol-gel method. The substrate was commercially available AA1050. The substrate

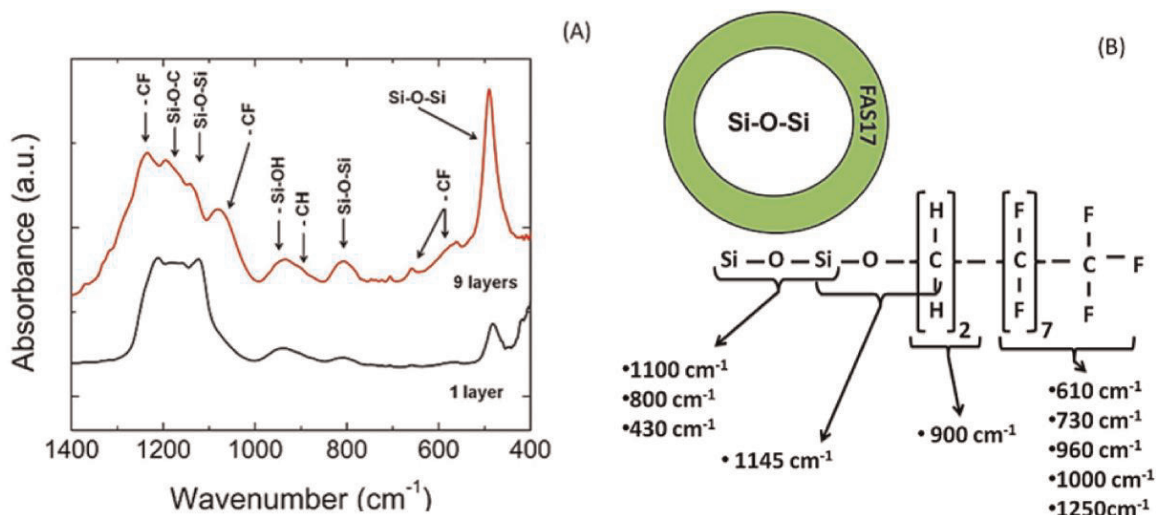


**Figure 19.** FTIR spectra of fluorinated silica nanoparticles coated on Al substrate as (A) a function of the number of layers and (B) schematic of the functionalized silica nanoparticle [55].

was first sanded and washed by acetone and then chemically etched to achieve micro roughness on the surface. Several approaches were compared to observe the effect of TEOS and GPTMS hybrid sol-gel coating containing functionalized  $\text{Al}_2\text{O}_3$  nanoparticles. They used functionalized nano- $\text{Al}_2\text{O}_3$  particles to improve surface micro- and nanoscale roughness and also improve mechanical properties of the superhydrophobic coating. In **Figure 20** the manufacturing process and WCA measurements are reported. In total four samples were compared to each other: (a) chemically etched and then functionalized in FAS solution without sol-gel coating, (b) chemically etched substrate dip coated by sol-gel hybrid coating and then functionalized by FAS solution, (c) addition of  $\text{Al}_2\text{O}_3$  to the hybrid sol-gel coating, and (d) addition of functionalized  $\text{Al}_2\text{O}_3$  to the sol-gel coating. Results showed that functionalized nanoparticles had a uniform dispersion in coating and fabricated a uniform hierarchical micro- and nanoscale roughness which is ideal for superhydrophobicity and also acted as a shield during abrasion cycles and protected from the surface and superhydrophobic properties after 200 abrasion cycles with a total length of 300 cm.

### 5.1.3. Electroless galvanic deposition

In this method, galvanic reactions are used to fabricate superhydrophobic coatings. The reaction starts with contact of metal ion with the surface of a metal with lower corrosion potential. The reaction would be spontaneous, so it is a low-cost and efficient method to make roughness on the surface of the metal. After this process, a low energy material is used to decrease the surface energy and achieve superhydrophobicity [67].

Xu et al. [68] fabricated a superhydrophobic feather-like silver coating on a copper substrate using electroless galvanic deposition method. The WCA was 169 and the sliding angle was 2. In **Figure 21**, the feather-like morphology of the silver coating is shown.

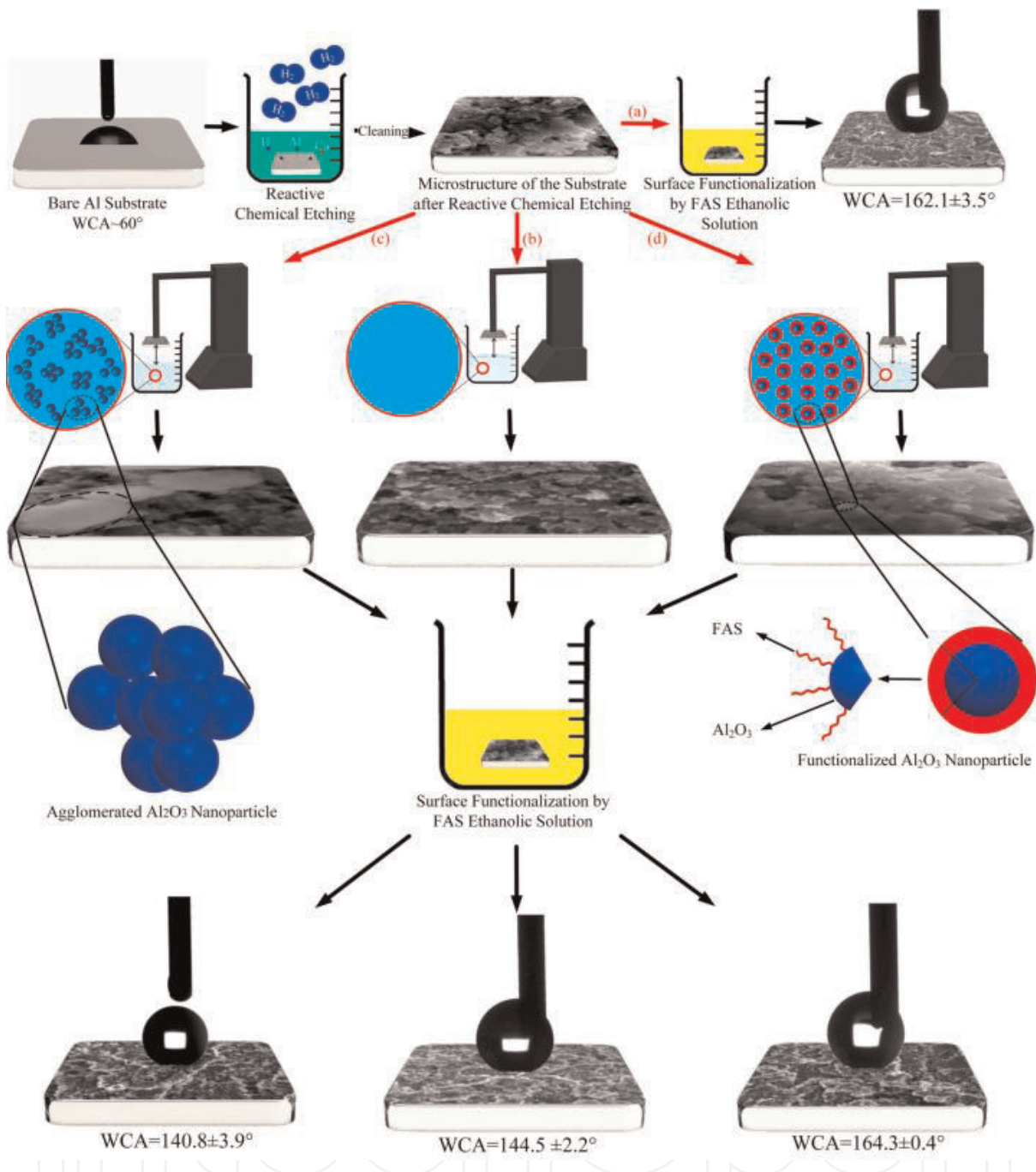


**Figure 20.** Schematics of superhydrophobic coating fabrication and investigation of functionalized and non-functionalized nanoparticles addition to sol-gel coating. Four samples are (a) aluminum substrate, which was chemically etched and then functionalized by FAS solution without any sol-gel coating, (b) the aluminum substrate after chemical etching was dip coated in TEOS-GPTMS hybrid sol-gel coating and the functionalized by FAS solution, (c) the same process was done by a hybrid TEOS-GPTMS coating containing  $\text{Al}_2\text{O}_3$  nanoparticles and (d) functionalized  $\text{Al}_2\text{O}_3$  nanoparticles were added to the coating and water contact measurements are reported [66].

#### 5.1.4. Electrodeposition

The electrodeposition method is one of the chemical-based methods used to achieve superhydrophobicity. The main advantages of this method are its low cost of production,

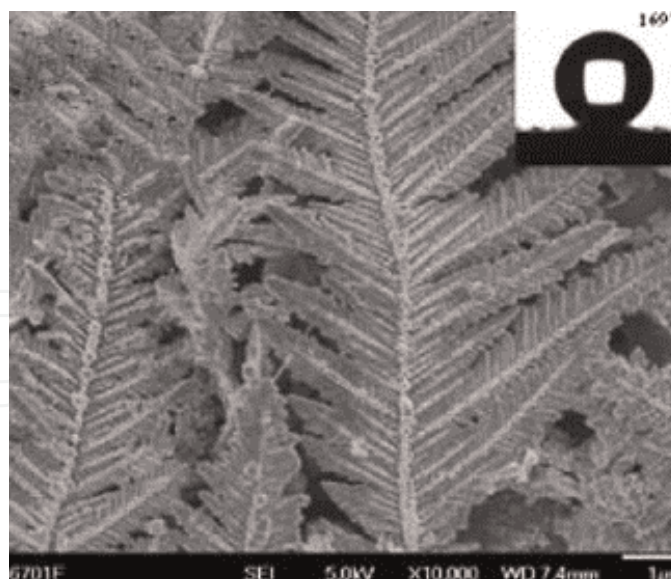


**Figure 21.** SEM image showing the feather-like morphology of superhydrophobic silver coating on copper substrate [68].

capability of large-scale production, being independent from the shape and size of the sample, and great uniformity. Although it is worth mentioning that the electrodeposition technique fabricates a hierarchical micro- and nanoscale roughness on the surface of metal and a low energy material is needed to be coated on the surface after electrodeposition to reduce surface energy. A combination of the hierarchical structure on the surface and lowered surface energy by low energy material coatings like lauric acid, stearic acid, fluoropolymers, etc. will lead to superhydrophobicity. Also, several studies have been reported that used a two-step electrodeposition technique to fabricate ideal hierarchical micro- and nanoscale roughness on the surface [69, 70].

Jain et al. [71] fabricated a superhydrophobic copper substrate by electrodeposition technique followed by low surface energy modifications in stearic acid. The WCA was  $162^\circ \pm 3^\circ$  and the sliding angle was about  $3^\circ$ . The copper substrate was chosen due to its wide application in industries. In **Figure 22**, SEM images of surface morphology and WCA are shown at different values of voltages including 0.5 V, 0.7 V, 0.9 V, and 1.1 V, showing the formation of globular asperities on the surface at potentials over 0.7 V.

The superhydrophobic surface fabricated by electrodeposition followed by stearic acid coating also showed self-cleaning properties. In **Figure 23**, superhydrophobic and ordinary surface are compared against an SiC particle dirt. As seen in the figure, the superhydrophobic sample cleaned completely by 55 drops of water.

In another study Xiang et al. [72] fabricated a superhydrophobic and superoleophilic mesh for oil-water separation using electrodeposition technique. The stainless-steel mesh was first washed and degreased by ethanol and then etched by 8 M HCl to remove the oxidation layer from the surface. The prepared mesh then put into solution consists of ethanol,  $\text{CuSO}_4$ ,  $\text{Na}_2\text{SO}_4$ ,  $\text{NiSO}_4$ , NDM, and dopamine hydrochloride, and the electrodeposition was done at

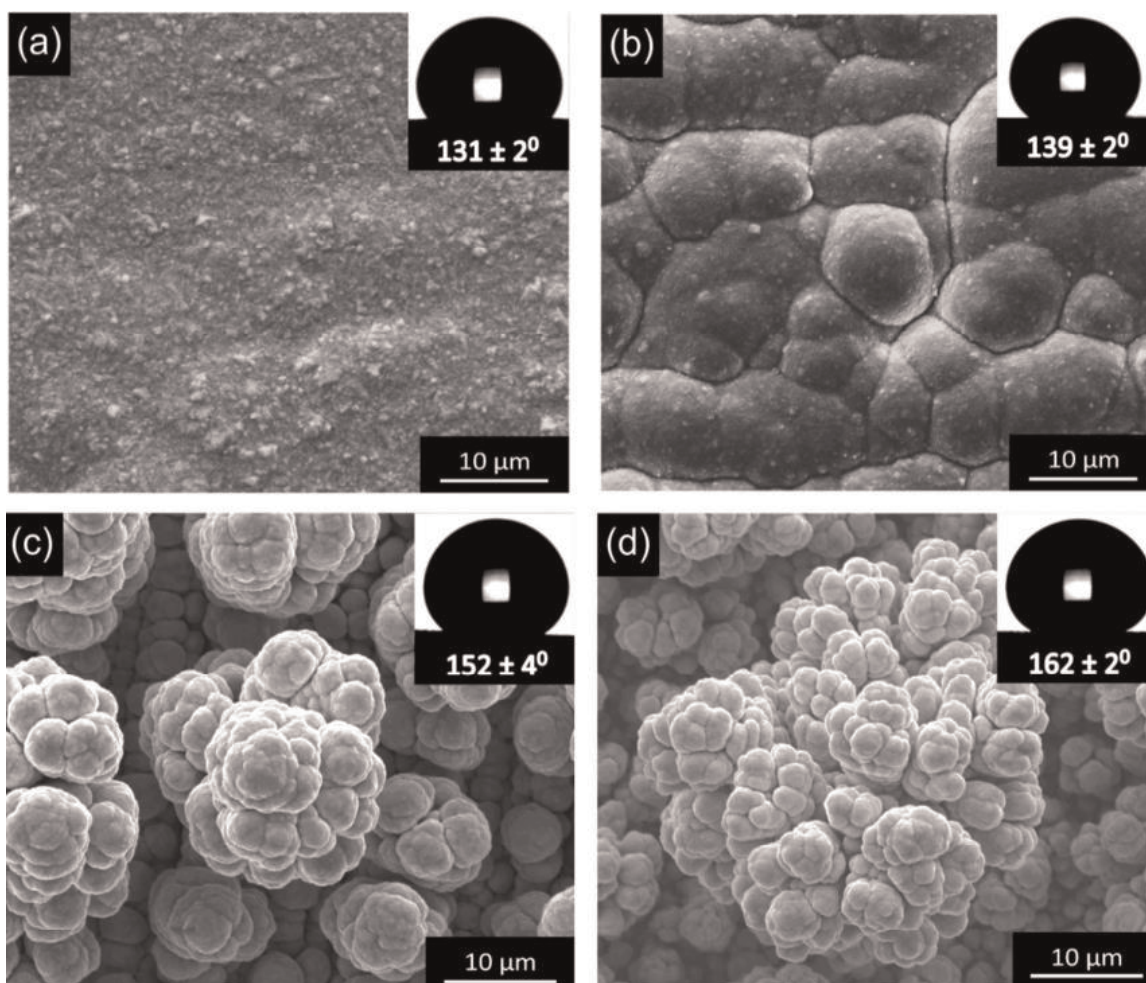


**Figure 22.** SEM images of surface morphology and WCA are shown at different values of voltages including 0.5 V, 0.7 V, 0.9 V, and 1.1 V [71].

0.6 A cm<sup>-2</sup> for 20 min. The result was a stainless-steel mesh with hierarchical micro- and nanoscale roughness as shown in **Figure 24**. The WCA was 162° and OCA<sup>3</sup> was 0°.

In **Figure 25**, a schematic of the final substrate after electrodeposition is shown. The Cu and Ni molecules are co-deposited by the conjugated pDOP-NDM. As mentioned before to achieve superhydrophobicity, hierarchical surface structure and low surface energy are needed at the same time. In this case, the pDOP-NDM molecules drastically reduced surface energy. Besides, the pDOP acts as a bonding agent which increases the bonding of Cu and Ni to the surface and also attaches them to the NDM. At last, the superhydrophobic and superoleophilic mesh had a high separation efficiency, good recyclability, and strong durability [72].

Su et al. [73] fabricated a robust abrasion and corrosion-resistant superhydrophobic coating on copper substrate by electrodeposition method. The nickel electrodeposition in this study was obtained through Watts bath consisting of NiSO<sub>4</sub>, NiCl<sub>2</sub>·6H<sub>2</sub>O, and H<sub>3</sub>BO<sub>3</sub>. The electrodeposition current density was 0.75 A cm<sup>-2</sup> and the duration time was 1 h. After that, the sample was

<sup>3</sup>Oil contact angle.

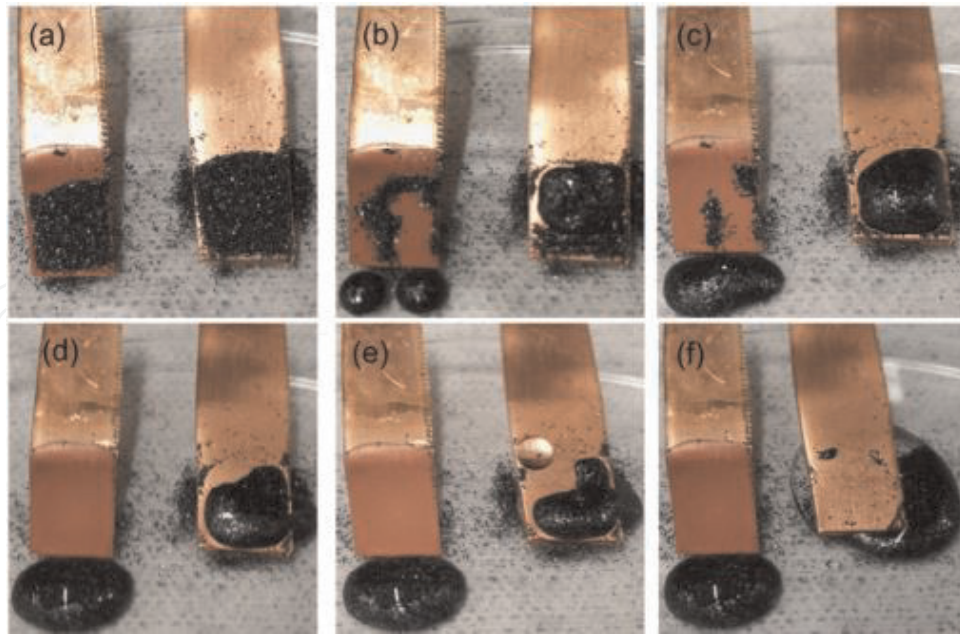


**Figure 23.** Self-cleaning properties of superhydrophobic copper substrate fabricated by electrodeposition method and compared to the ordinary substrate (a) dirty samples by SiC particles, (b) 2, (c) 5, (d) 10, (e) 30, and (f) 55 drops of water.

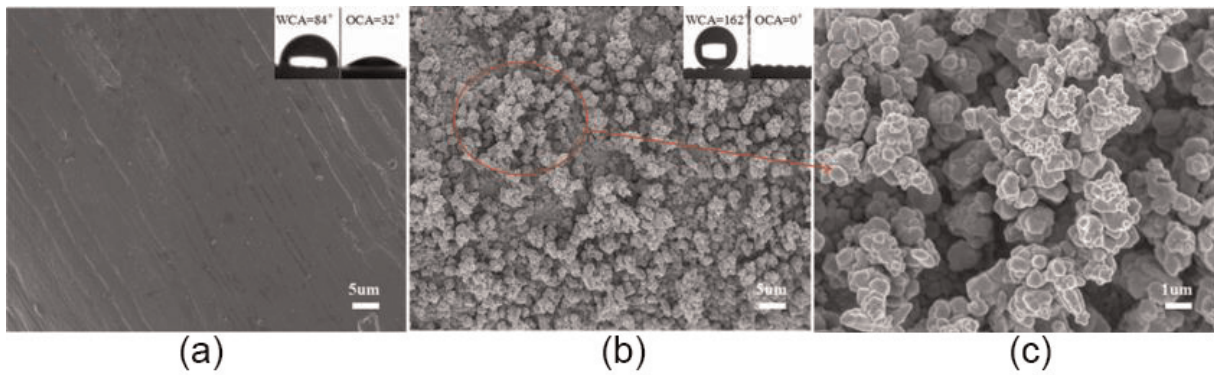


**Figure 24.** WCA and OCA on stainless steel substrate before (a) and after (b and c) electrodeposition process [72].

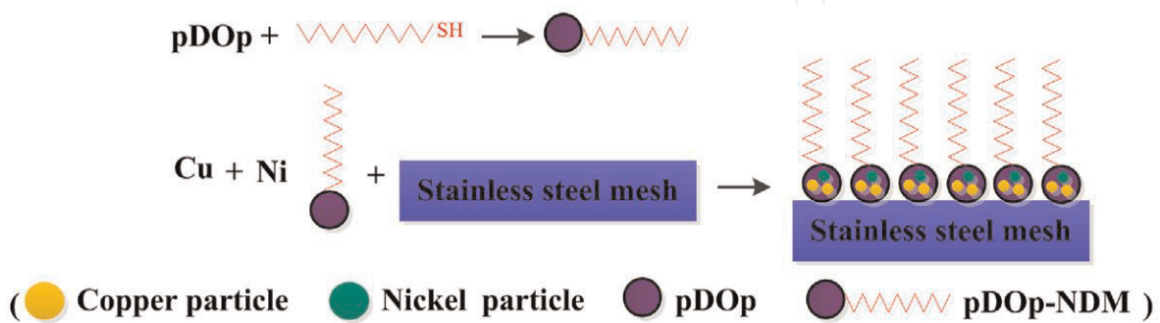


**Figure 25.** The conjugated pDOP-NDM anchored on Cu and nucleus [72].

put into a sealed reactor containing AC-FAS ethanol solution for 1 h at 110°C. In **Figure 26**, the schematic of the coating process is shown.

The nickel coating on top provided a hierarchical structure on surface, and AC-FAS lowered the surface energy resulted in superhydrophobic properties with good mechanical properties and high corrosion resistance. In **Figure 27**, Nyquist and bode plots of pure copper substrate, electrodeposited Ni, and superhydrophobic surface are shown in which the superhydrophobic surface has much higher corrosion resistance [73].

#### 5.1.5. Chemical functionalization

Wu et al. [74] fabricated a ZnO-based surface on a glass slide in which a layer of ZnO was first deposited on the substrate, and then self-assembled monolayers<sup>4</sup> were used to lower surface energy and achieve superhydrophobic properties. In **Figure 28**, the microstructure of the ZnO coating on the substrate is shown. The hierarchical micro- and nanoroughness of the ZnO coating followed by low surface energy treatment will lead to superhydrophobic properties.

Xu et al. [74] fabricated a superhydrophobic nanocomposite TiO<sub>2</sub>/polystyrene coating which can be deposited through simple spray coating. TiO<sub>2</sub> nanoparticles were first functionalized by PFOA and then added to the polystyrene matrix and deposited on the substrate by spraying. It was found that usage of equal amounts of functionalized TiO<sub>2</sub> and polystyrene led into optimum superhydrophobic properties with WCA of 166°.

Wang et al. [74] fabricated a superhydrophobic surface on PDMS using modified ZnO particles. The ZnO particles were fabricated through a CVD process, and then they were functionalized to reduce the chance of agglomeration. In **Figure 29**, as-prepared ZnO rods are shown which are greatly suitable to form hierarchical micro- and nanoscale roughness. Also, coating WCA and microstructure are shown.

Wu et al. [75] fabricated a superhydrophobic coating by simply adding functionalized silica nanoparticles. The silica nanoparticles are first added to an ethanol solution containing PTES to

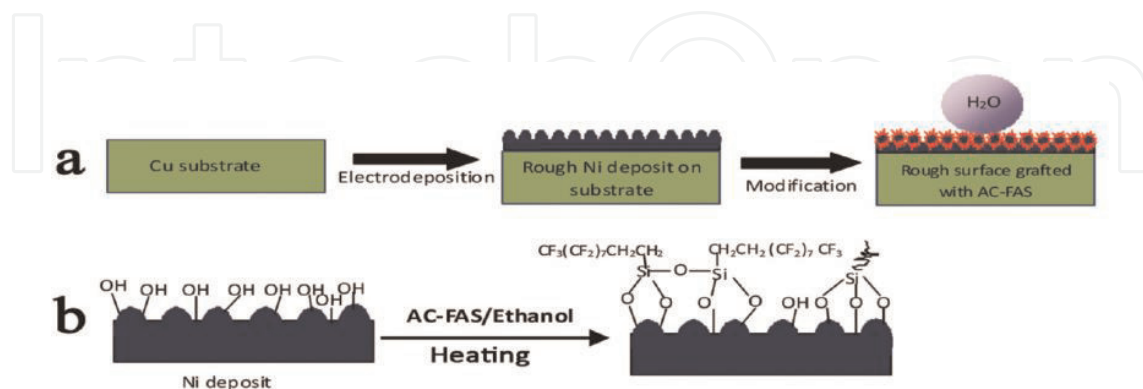


**Figure 26.** Schematics of Cu substrate electrodeposited by Ni followed by AC-FAS treatment [73].

<sup>4</sup>SAMs.

form hydrophobic silica particles, and then they were added to the epoxy to form the nanocomposite coating. As shown in **Figure 30**, the coating deposition of the substrate is not limited to only one method, and it can be brushed, dipped, and sprayed to the substrate.

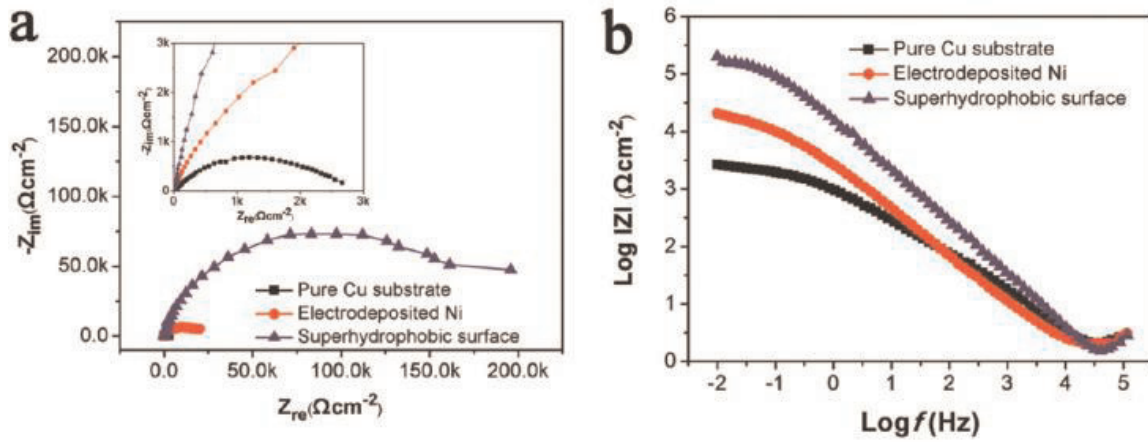


**Figure 27.** Nyquist and bode plots of pure Cu substrate, electrodeposited Ni, and superhydrophobic surface [73].

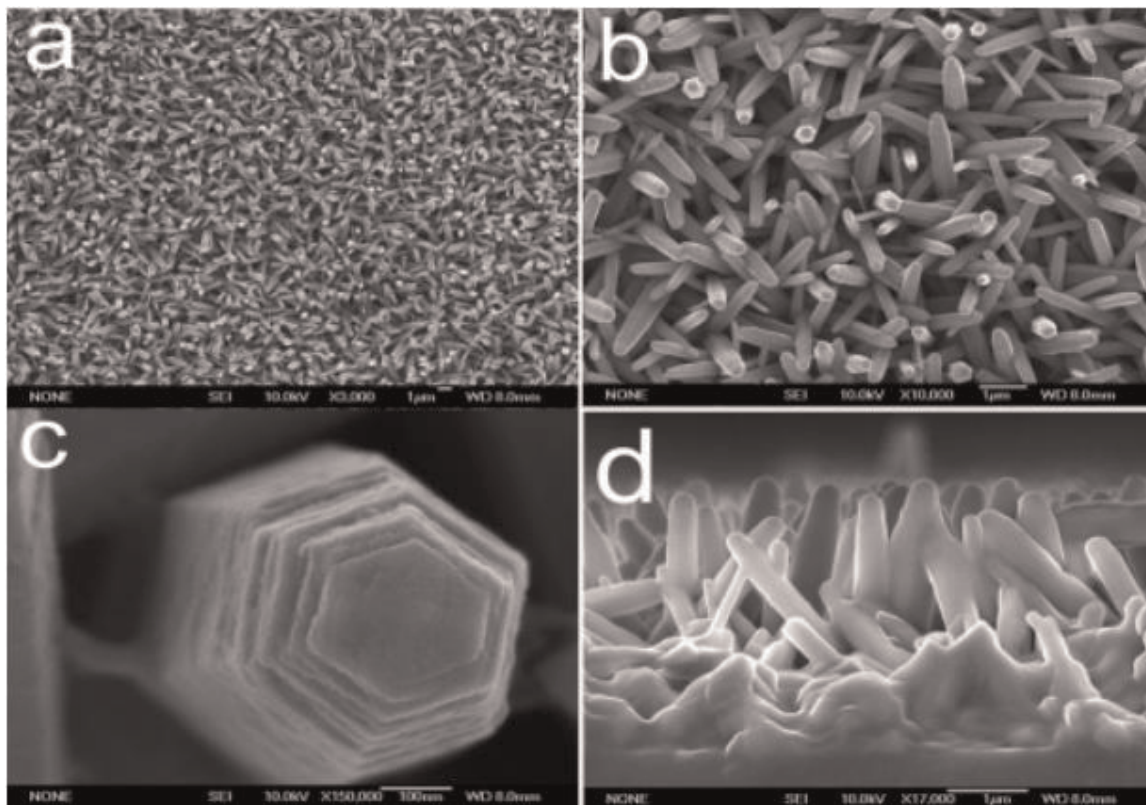


**Figure 28.** FESEM image of the surface at (a) low magnification, (b) high magnification, (c) hexagonal nanorod, and (d) cross-sectional view [74].

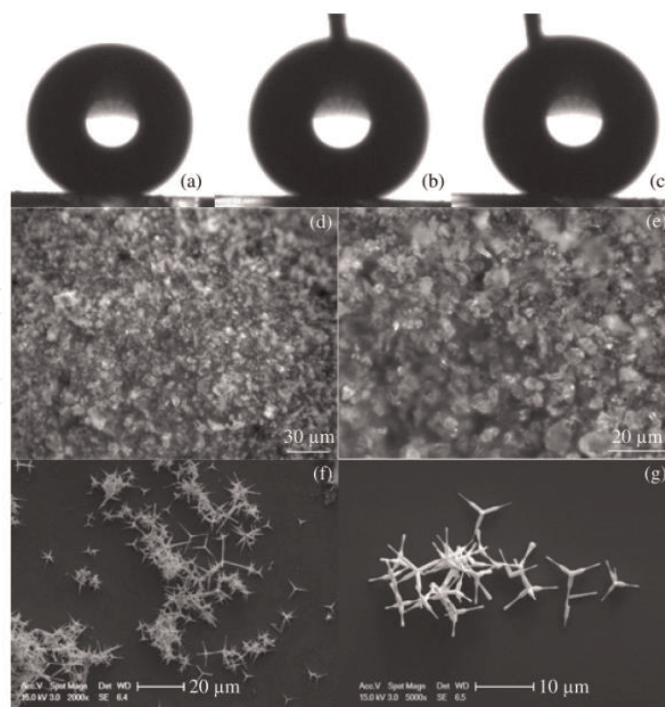


**Figure 29.** (a, b, c) WCA, advancing and receding angles, (d, e) coating microstructure, (f and g) as-prepared ZnO rods [74].

## 5.2. Lithography

The lithography method is one of the well-known processes used to fabricate superhydrophobic coatings. This method includes light-assisted, soft, nano-, electron beam-assisted, X-ray, and colloidal lithography. In this method, superhydrophobic surface is generally made using a soft or hard surface as a reference and makes a new surface by copying the reference surface [76]. Different methods of lithography are not independent of each other, and it is possible to use two methods of lithography during the fabrication process. For example, light-assisted lithography is used during nanolithography [77].

Before in traditional lithography, a smooth surface was used as a reference, but now in the photolithography process, all the details of surface roughness can be identified by the use of X-ray and a photosensitive thin film. In soft lithography also an elastomer material is used for molding the surface, and then that is used for templating from the surface [78].

## 5.3. Templating

Templating method is one of the methods to fabricate superhydrophobic surfaces in which usually lithography method is used to build a template from the reference surface, and then that template will be used for templating procedure. The template surface can be a paper filter, insect wing, some animal's skin, and plant leaf. From the chemical and morphological aspect, the template can even be a molecule or polymer [79, 80].

In general, this method includes making a template and molding from that and then building a surface by using that mold (see **Figure 31**). One of the ways to build a superhydrophobic

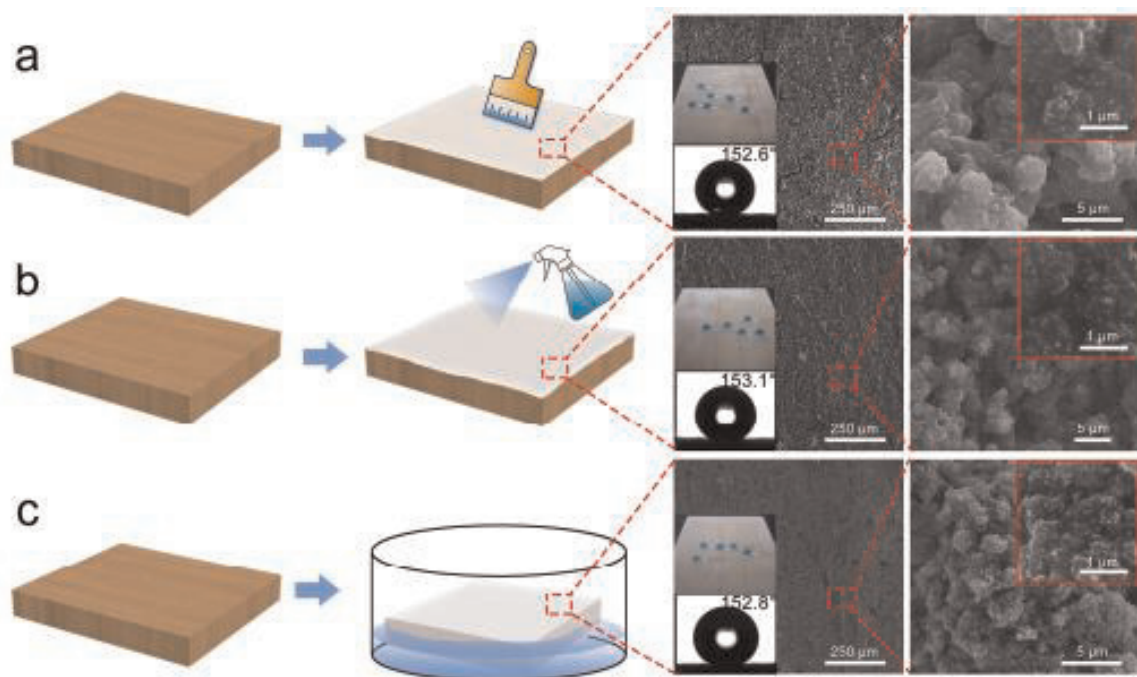


**Figure 30.** Superhydrophobic nanocomposite coating deposited on substrate through different methods and their microstructure and WCA measurements [75].

surface is to use gecko's feet as a template [81]. In **Figure 31**, the templating procedure from the lotus leaf is shown; in this procedure, first the lotus leaf is fixed on a prepared holder, and this leaf is coated with gold, and a nickel mold is used to build a mold from the lotus leaf.

#### 5.4. Chemical vapor deposition

This method includes deposition of gas on substrate by chemical reactions. To evaporate the material in the CVD process, plasma, laser, catalysts, etc. can be used to ease the process. Some works that have used this method to achieve superhydrophobic properties will be mentioned here. Borrás et al. [83] used plasma-assisted CVD to achieve superhydrophobicity by Ag-TiO<sub>2</sub> nanofibers on the surface of the substrate. The fibers included an Ag core wrapped with a TiO<sub>2</sub> shell. The water contact angle of the surface depended on the shape of the fibers and space between them. In the best situation, WCA was reached to near 180°. In superhydrophobic coatings with TiO<sub>2</sub> and ZnO, a change in wetting properties from superhydrophobic to superhydrophilic through UV irradiation can be observed. The reason for this unexpected change in wetting behavior is that UV irradiation will cause electron-hole pairs on the surface which will react with the lattice oxygen, and this will cause oxygen vacancy on the surface. These oxygen vacancies cause the water molecules to easily bond with the surface, and as a result, WCA will be drastically reduced to near zero.

In another study, Jung and Bhushan [84] fabricated multi-walled CNT by catalyst-assisted CVD and then combined that with resin and sprayed it on the Si substrate with microstructural roughness. The WCA of the surface was 170° and the CAH was about 2°. The superhydrophobic properties were stable in this sample and showed good results after long exposure to water.

Many other studies have used CVD to fabricate superhydrophobic coating, but the process is very complicated, and it is not possible to control the resulting surface morphology completely.

### 5.5. Layer-by-layer deposition

This method is an easier method than CVD and plasma which does not need very special equipment. In this method, several layers of thin coating will be applied on the substrate by changing the electrical charge, and there is less limitation in the size of the sample than CVD. Layer-by-layer deposition is a relatively easy method to fabricate a hierarchical structure on the substrate. Usually, some nanoparticle additives are used to improve the surface roughness. Cohen and Rubner's group [85, 86] used this method to fabricate superhydrophobic coatings. They used different kinds of solutions to fabricate three layers of the coating including adhesion, body, and top layer. In **Figure 32**, the schematic of the LBL process shows three solutions, consisting of polyallylamine hydrochloride<sup>5</sup>, sodium 4-styrenesulfonate<sup>6</sup>, and silica particles.

### 5.6. Colloidal aggregation and assembling

This method is usually used to ease sol-gel, chemical deposition, and lithography processes to fabricate hierarchical micro- and nanoscale roughness. In this method, chemical and van der Waals bond between the dispersed particles and deposition of these particles on the surface will make a multilayer rough surface [87]. To fabricate these kinds of multilayer rough surface, immersion or spin coating is used. For example, Min et al. [88] fabricated colloidal particles with a controlled size of 70 nm which were possible to deposit on large surfaces using a spin coating method. In **Figure 33a**, the TEM image of synthesized silica nanoparticles is shown. In **Figure 33b**, the SEM image of coating surface structure after deposition on the substrate by spin coating with 10,000 rpm and for 10 minutes is shown. The thickness of the crystalline colloidal layer can be controlled by the speed and time of the spin coating process.

### 5.7. Electrospinning and electrospraying

These two methods are similar to each other and are used to fabricate micro- or nano-structures. The electrospinning method is an easy way to fabricate continuous polymer fibers in micro- and nanoscale [89]. This method is suitable to make a roughened surface needed to achieve superhydrophobicity on the surface [90]. To produce uniform fibers, polymer molecular weight and solution concentration should be controlled [91].

On the other hand, the electrospraying method is not just limited to fibers, and the deposited polymer film can have different shapes from spheres to fibers [92]. Generally, polymeric fibers are produced through electrospinning, and films consist of spherical seeds, which are fabricated by electrospraying method [93].

---

<sup>5</sup>PAH.

<sup>6</sup>SPS.

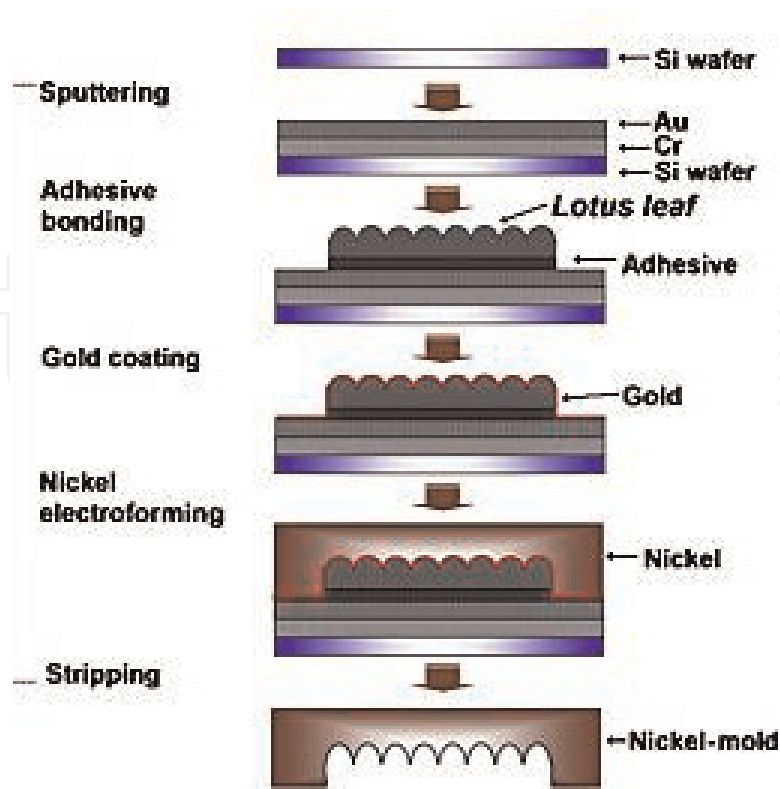


Figure 31. Schematics of the templating procedure from lotus leaf [82].

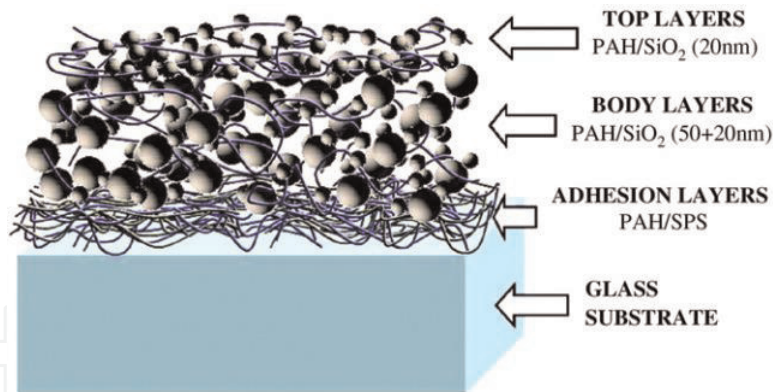
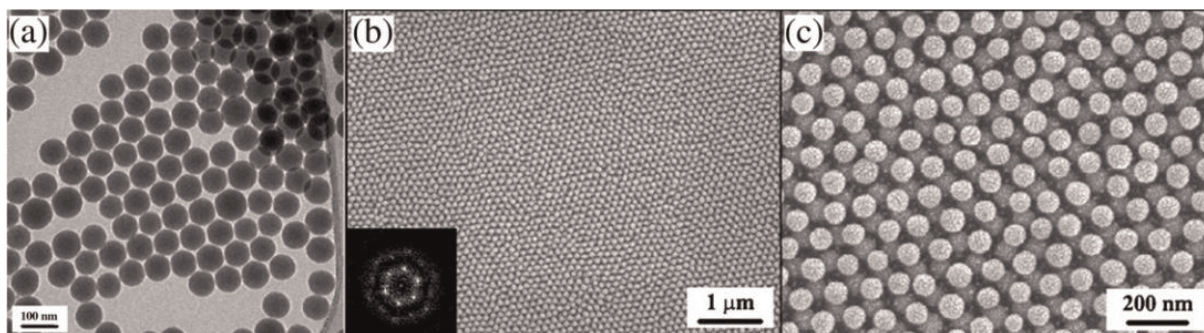


Figure 32. Schematic of the LBL method used to fabricate superhydrophobic coating [85].

Ding et al. [94] fabricated superhydrophobic nanostructured ZnO coating by the electrospinning method. The composite coating consisted of polyvinyl alcohol<sup>7</sup> and ZnO nanofibers. After that to reduce surface energy, fluoroalkyl silane was used to modify the surface and lower the energy on the surface, and superhydrophobicity was achieved. The FESEM image of inorganic ZnO fibers is shown in **Figure 34**. Before surface modification with

<sup>7</sup>PVA.



**Figure 33.** (a) TEM image of synthesized silica nanoparticles, (b, c) SEM image of the coating surface structure on substrate [88].

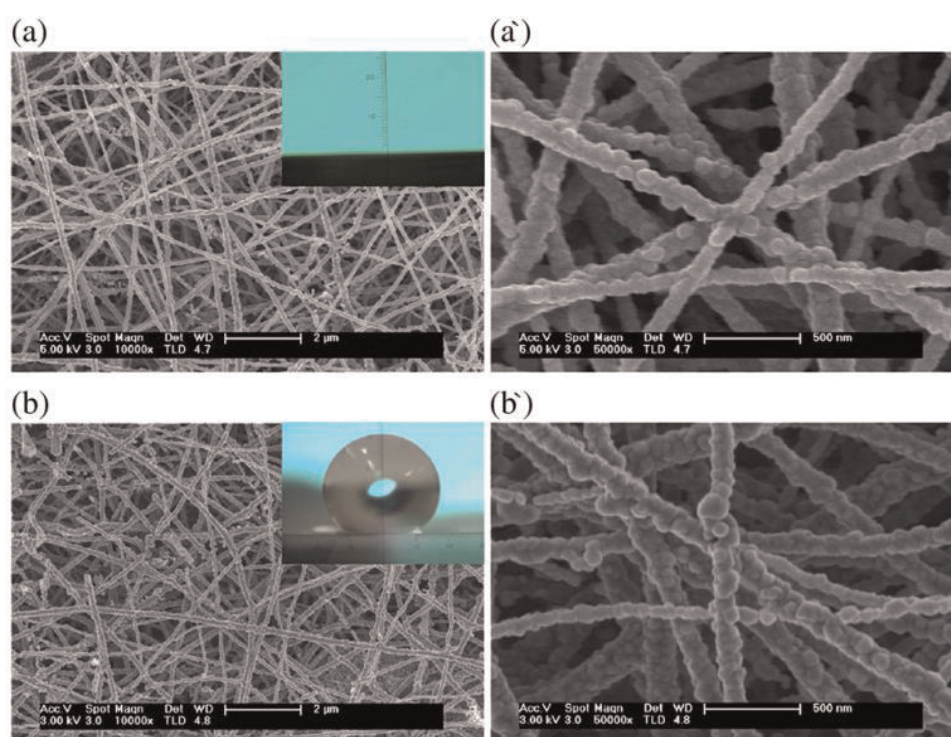


**Figure 34.** FESEM image of ZnO fibers film (a, a') before modification and (b, b') after modification [94].

fluoroalkyl silane, WCA was  $0^\circ$ , and the surface was superhydrophilic, but after surface modification, the WCA was  $165^\circ$ , and the sliding angle was  $5^\circ$ .

Burkarter et al. [95] fabricated a PTFE film by electrospay method on a glass substrate which had a fluorine-doped tin oxide coating. The result was a superhydrophobic coating with WCA equal to  $160^\circ$  and a sliding angle less than  $2^\circ$ . Actually, the electrospay method used in this study was very similar to the electrospinning, but because there was no need for PTFE fiber, then the electrospay method was used. The SEM image of hierarchical micro- and nanoscale roughness of the coating is shown in **Figure 35**.

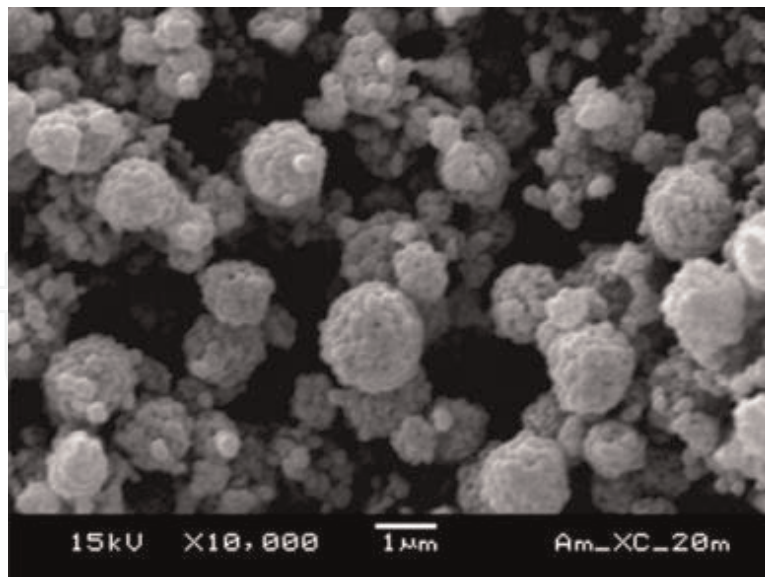


**Figure 35.** SEM image of hierarchical micro- and nanoscale roughness of PTFE film deposited by electrospray method on a glass substrate which had a fluorine-doped tin oxide coating [95].

### 5.8. Phase separation

In this method, a surface pattern is made by separation solid phase from a semi-stable mixture by changing the temperature, pressure, or other environmental conditions. Phase separation method can also be involved in colloidal assembling. The surface structure in this method can be in macro-, micro-, or nanoscale [96]. This method is usually followed by sol-gel method to control resulted surface pattern [97]. Phase separation method can also be followed by other methods like plasma treatment, electrospinning, and self-aggregation to achieve superhydrophobicity. The phase separation method is partially related to colloidal polymerization [98].

## 6. Drawbacks of superhydrophobic coatings

There have been many improvements in the case of superhydrophobic coating fabrication and their stability, but there is still room to grow. Many studies on the superhydrophobic coatings do not consider mechanical properties as their focus or at least part of the study. Many of superhydrophobic coatings have poor bonding either to the substrate or to itself. Also, many other superhydrophobic coatings will lose their special wetting behavior during long-term use or in harsh environments. Also, almost in most superhydrophobic coatings, a low surface energy treatment is done, which does not have suitable bonding and stability on coating substrate and, in the case of fluorine-based materials, is toxic and harmful for environments. These weak points have hindered industrial application of superhydrophobic coatings.

## Author details

Sepehr Shadmani<sup>1</sup>, Mehdi Khodaei<sup>1\*</sup>, Xiuyong Chen<sup>2,3</sup> and Hua Li<sup>2,3</sup>

\*Address all correspondence to: khodaei@kntu.ac.ir

1 Faculty of Materials Science and Engineering, K.N. Toosi University of Technology, Tehran, Iran

2 Key Laboratory of Marine Materials and Related Technologies, Zhejiang Key Laboratory of Marine Materials and Protective Technologies, Ningbo Institute of Materials Technology and Engineering, Chinese Academy of Sciences, Ningbo, China

3 Cixi Institute of Biomedical Engineering, Ningbo Institute of Materials Technology and Engineering, Chinese Academy of Sciences, Ningbo, China

## References

- [1] Goodwyn PP, Maezono Y, Hosoda N, Fujisaki K. Waterproof and translucent wings at the same time: Problems and solutions in butterflies. *Naturwissenschaften*. 2009;**96**:781-787
- [2] Gao X, Jiang L. Water-repellent legs of water striders. *Nature*. 2004;**432**:36-36
- [3] Das S, Kumar S, Samal SK, Mohanty S, Nayak SK. A review on superhydrophobic polymer nanocoatings: Recent development and applications. *Industrial & Engineering Chemistry Research*. 2018;**57**:2727-2745
- [4] Gao L, McCarthy TJ. Contact angle hysteresis explained. *Langmuir*. 2006;**22**:6234-6237
- [5] Hao P, Lv C, Yao Z, He F. Sliding behavior of water droplet on superhydrophobic surface. *Europhysics Letters*. 2010;**90**:66003
- [6] Wang B, Liang W, Guo Z, Liu W. Biomimetic super-lyophobic and super-lyophilic materials applied for oil/water separation: A new strategy beyond nature. *Chemical Society Reviews*. 2015;**44**:336-361
- [7] Gao C, Sun Z, Li K, Chen Y, Cao Y, Zhang S, et al. Integrated oil separation and water purification by a double-layer TiO<sub>2</sub>-based mesh. *Energy & Environmental Science*. 2013;**6**: 1147-1151
- [8] Crick CR, Gibbins JA, Parkin IP. Superhydrophobic polymer-coated copper-mesh; membranes for highly efficient oil-water separation. *Journal of Materials Chemistry A*. 2013;**1**: 5943-5948
- [9] Nguyen DD, Tai N-H, Lee S-B, Kuo W-S. Superhydrophobic and superoleophilic properties of graphene-based sponges fabricated using a facile dip coating method. *Energy & Environmental Science*. 2012;**5**:7908-7912

- [10] Zhu Q, Chu Y, Wang Z, Chen N, Lin L, Liu F, et al. Robust superhydrophobic polyurethane sponge as a highly reusable oil-absorption material. *Journal of Materials Chemistry A*. 2013;**1**:5386-5393
- [11] Zhang Y-L, Xia H, Kim E, Sun H-B. Recent developments in superhydrophobic surfaces with unique structural and functional properties. *Soft Matter*. 2012;**8**:11217-11231
- [12] Fan Y, Li C, Chen Z, Chen H. Study on fabrication of the superhydrophobic sol-gel films based on copper wafer and its anti-corrosive properties. *Applied Surface Science*. 2012;**258**:6531-6536
- [13] Ishizaki T, Sakamoto M. Facile formation of biomimetic color-tuned superhydrophobic magnesium alloy with corrosion resistance. *Langmuir*. 2011;**27**:2375-2381
- [14] Xu W, Song J, Sun J, Lu Y, Yu Z. Rapid fabrication of large-area, corrosion-resistant superhydrophobic Mg alloy surfaces. *ACS Applied Materials & Interfaces*. 2011;**3**:4404-4414
- [15] Tian Y, Su B, Jiang L. Interfacial material system exhibiting superwettability. *Advanced Materials*. 2014;**26**:6872-6897
- [16] de Leon ACC, Pernites RB, Advincula RC. Superhydrophobic colloiddally textured polythiophene film as superior anticorrosion coating. *ACS Applied Materials & Interfaces*. 2012;**4**:3169-3176
- [17] Wang N, Xiong D. Superhydrophobic membranes on metal substrate and their corrosion protection in different corrosive media. *Applied Surface Science*. 2014;**305**:603-608
- [18] Gnedenkov S, Egorkin V, Sinebryukhov S, Vyaliy I, Pashinin A, Emelyanenko A, et al. Formation and electrochemical properties of the superhydrophobic nanocomposite coating on PEO pretreated Mg-Mn-Ce magnesium alloy. *Surface and Coatings Technology*. 2013;**232**:240-246
- [19] Cheng J, Zhang J, Liu F. Recent development of metal hydroxides as electrode material of electrochemical capacitors. *RSC Advances*. 2014;**4**:38893-38917
- [20] Chen X, Yuan J, Huang J, Ren K, Liu Y, Lu S, et al. Large-scale fabrication of superhydrophobic polyurethane/nano- $\text{Al}_2\text{O}_3$  coatings by suspension flame spraying for anti-corrosion applications. *Applied Surface Science*. 2014;**311**:864-869
- [21] Wang G, Guo Z, Liu W. Interfacial effects of superhydrophobic plant surfaces: A review. *Journal of Bionic Engineering*. 2014;**11**:325-345
- [22] Tung WS, Daoud WA. Self-cleaning fibers via nanotechnology: A virtual reality. *Journal of Materials Chemistry*. 2011;**21**:7858-7869
- [23] Gao L, McCarthy TJ. Wetting  $101^\circ$ . *Langmuir*. 2009;**25**:14105-14115
- [24] Ho AYY, Luong Van E, Lim CT, Natarajan S, Elmouelhi N, Low HY, et al. Lotus bioinspired superhydrophobic, self-cleaning surfaces from hierarchically assembled templates. *Journal of Polymer Science Part B: Polymer Physics*. 2014;**52**:603-609

- [25] Daoud WA, editor. *Self-Cleaning Materials and Surfaces: A Nanotechnology Approach*. NYC, USA: John Wiley & Sons; Jul 12 2013
- [26] Wisdom KM, Watson JA, Qu X, Liu F, Watson GS, Chen C-H. Self-cleaning of superhydrophobic surfaces by self-propelled jumping condensate. *Proceedings of the National Academy of Sciences*. 2013;**110**:7992-7997
- [27] Meuler AJ, McKinley GH, Cohen RE. Exploiting topographical texture to impart icephobicity. *ACS Nano*. 2010;**4**:7048-7052
- [28] Guo P, Zheng Y, Wen M, Song C, Lin Y, Jiang L. Icephobic/anti-icing properties of micro/nanostructured surfaces. *Advanced Materials*. 2012;**24**:2642-2648
- [29] Peng C, Xing S, Yuan Z, Xiao J, Wang C, Zeng J. Preparation and anti-icing of superhydrophobic PVDF coating on a wind turbine blade. *Applied Surface Science*. 2012; **259**:764-768
- [30] Boinovich L, Emelyanenko AM. Role of water vapor desublimation in the adhesion of an iced droplet to a superhydrophobic surface. *Langmuir*. 2014;**30**:12596-12601
- [31] Li X-M, Reinhoudt D, Crego-Calama M. What do we need for a superhydrophobic surface? A review on the recent progress in the preparation of superhydrophobic surfaces. *Chemical Society Reviews*. 2007;**36**:1350-1368
- [32] Richard D, Quéré D. Bouncing water drops. *Europhysics Letters*. 2000;**50**:769
- [33] Wang Y, Xue J, Wang Q, Chen Q, Ding J. Verification of icephobic/anti-icing properties of a superhydrophobic surface. *ACS Applied Materials & Interfaces*. 2013;**5**:3370-3381
- [34] Sohn Y, Kim D, Lee S, Yin M, Song JY, Hwang W, et al. Anti-frost coatings containing carbon nanotube composite with reliable thermal cyclic property. *Journal of Materials Chemistry A*. 2014;**2**:11465-11471
- [35] Wang Y, Li M, Lv T, Wang Q, Chen Q, Ding J. Influence of different chemical modifications on the icephobic properties of superhydrophobic surfaces in a condensate environment. *Journal of Materials Chemistry A*. 2015;**3**:4967-4975
- [36] Hejazi V, Sobolev K, Nosonovsky M. From superhydrophobicity to icephobicity: Forces and interaction analysis. *Scientific Reports*. 2013;**3**:2194
- [37] McHale G, Newton MI, Shirtcliffe NJ. Immersed superhydrophobic surfaces: Gas exchange, slip and drag reduction properties. *Soft Matter*. 2010;**6**:714-719
- [38] Bhushan B. Bioinspired structured surfaces. *Langmuir*. 2012;**28**:1698-1714
- [39] Su B, Li M, Lu Q. Toward understanding whether superhydrophobic surfaces can really decrease fluidic friction drag. *Langmuir*. 2009;**26**:6048-6052
- [40] Watanabe K, Udagawa Y, Udagawa H. Drag reduction of Newtonian fluid in a circular pipe with a highly water-repellent wall. *Journal of Fluid Mechanics*. 1999;**381**:225-238

- [41] Moaven K, Rad M, Taeibi-Rahni M. Experimental investigation of viscous drag reduction of superhydrophobic nano-coating in laminar and turbulent flows. *Experimental Thermal and Fluid Science*. 2013;**51**:239-243
- [42] Deng Z-Y, Wang W, Mao L-H, Wang C-F, Chen S. Versatile superhydrophobic and photocatalytic films generated from TiO<sub>2</sub>-SiO<sub>2</sub>@ PDMS and their applications on fabrics. *Journal of Materials Chemistry A*. 2014;**2**:4178-4184
- [43] Dong H, Cheng M, Zhang Y, Wei H, Shi F. Extraordinary drag-reducing effect of a superhydrophobic coating on a macroscopic model ship at high speed. *Journal of Materials Chemistry A*. 2013;**1**:5886-5891
- [44] Rothstein JP. Slip on superhydrophobic surfaces. *Annual Review of Fluid Mechanics*. 2010;**42**:89-109
- [45] Banerjee I, Pangule RC, Kane RS. Antifouling coatings: Recent developments in the design of surfaces that prevent fouling by proteins, bacteria, and marine organisms. *Advanced Materials*. 2011;**23**:690-718
- [46] Schierholz J, Beuth J. Implant infections: A haven for opportunistic bacteria. *Journal of Hospital Infection*. 2001;**49**:87-93
- [47] Hetrick EM, Schoenfisch MH. Reducing implant-related infections: Active release strategies. *Chemical Society Reviews*. 2006;**35**:780-789
- [48] Guo Z, Zhou F, Hao J, Liu W. Stable biomimetic super-hydrophobic engineering materials. *Journal of the American Chemical Society*. 2005;**127**:15670-15671
- [49] Heinonen S, Huttunen-Saarivirta E, Nikkanen J-P, Raulio M, Priha O, Laakso J, et al. Antibacterial properties and chemical stability of superhydrophobic silver-containing surface produced by sol-gel route. *Colloids and Surfaces A: Physicochemical and Engineering Aspects*. 2014;**453**:149-161
- [50] Xue C-H, Chen J, Yin W, Jia S-T, Ma J-Z. Superhydrophobic conductive textiles with antibacterial property by coating fibers with silver nanoparticles. *Applied Surface Science*. 2012;**258**:2468-2472
- [51] Song J, Xu W, Liu X, Lu Y, Wei Z, Wu L. Ultrafast fabrication of rough structures required by superhydrophobic surfaces on Al substrates using an immersion method. *Chemical Engineering Journal*. 2012;**211**:143-152
- [52] Ma W, Wu H, Higaki Y, Otsuka H, Takahara A. A "non-sticky" superhydrophobic surface prepared by self-assembly of fluoroalkyl phosphonic acid on a hierarchically micro/nano-structured alumina gel film. *Chemical Communications*. 2012;**48**:6824-6826
- [53] Mahadik SA, Kavale MS, Mukherjee S, Rao AV. Transparent superhydrophobic silica coatings on glass by sol-gel method. *Applied Surface Science*. 2010;**257**:333-339
- [54] Kim E-K, Lee C-S, Kim SS. Superhydrophobicity of electrospray-synthesized fluorinated silica layers. *Journal of Colloid and Interface Science*. 2012;**368**:599-602

- [55] Brassard J-D, Sarkar DK, Perron J. Fluorine based superhydrophobic coatings. *Applied Sciences*. 2012;**2**:453-464
- [56] Brassard J-D, Sarkar DK, Perron J. Synthesis of monodisperse fluorinated silica nanoparticles and their superhydrophobic thin films. *ACS Applied Materials & Interfaces*. 2011;**3**:3583-3588
- [57] Huang Y, Sarkar DK, Chen X-G. A one-step process to engineer superhydrophobic copper surfaces. *Materials Letters*. 2010;**64**:2722-2724
- [58] Safaee A, Sarkar DK, Farzaneh M. Superhydrophobic properties of silver-coated films on copper surface by galvanic exchange reaction. *Applied Surface Science*. 2008;**254**:2493-2498
- [59] Saleema N, Sarkar DK, Gallant D, Paynter RW, Chen X-G. Chemical nature of superhydrophobic aluminum alloy surfaces produced via a one-step process using fluoroalkyl-silane in a base medium. *ACS Applied Materials & Interfaces*. 2011;**3**:4775-4781
- [60] Sarkar DK, Farzaneh M, Paynter RW. Superhydrophobic properties of ultrathin rf-sputtered Teflon films coated etched aluminum surfaces. *Materials Letters*. 2008;**62**:1226-1229
- [61] Sarkar DK, Saleema N. One-step fabrication process of superhydrophobic green coatings. *Surface and Coatings Technology*. 2010;**204**:2483-2486
- [62] Teshima K, Sugimura H, Inoue Y, Takai O. Gas barrier performance of surface-modified silica films with grafted organosilane molecules. *Langmuir*. 2003;**19**:8331-8334
- [63] Zhao Y, Li M, Lu Q, Shi Z. Superhydrophobic polyimide films with a hierarchical topography: Combined replica molding and layer-by-layer assembly. *Langmuir*. 2008;**24**:12651-12657
- [64] Hozumi A, Takai O. Effect of hydrolysis groups in fluoro-alkyl silanes on water repellency of transparent two-layer hard-coatings. *Applied Surface Science*. 1996;**103**:431-441
- [65] Latthe SS, Imai H, Ganesan V, Rao AV. Superhydrophobic silica films by sol-gel coprecursor method. *Applied Surface Science*. 2009;**256**:217-222
- [66] Khodaei M, Shadmani S. Superhydrophobicity on aluminum through reactive-etching and TEOS/GPTMS/nano-Al<sub>2</sub>O<sub>3</sub> silane-based nanocomposite coating. *Surface and Coatings Technology*. 2019;**374**:1078-1090
- [67] Gu C, Zhang T-Y. Electrochemical synthesis of silver polyhedrons and dendritic films with superhydrophobic surfaces. *Langmuir*. 2008;**24**:12010-12016
- [68] Xu X, Zhang Z, Yang J. Fabrication of biomimetic superhydrophobic surface on engineering materials by a simple electroless galvanic deposition method. *Langmuir*. 2009;**26**:3654-3658

- [69] Haghdoost A, Pitchumani R. Fabricating superhydrophobic surfaces via a two-step electrodeposition technique. *Langmuir*. 2014;**30**:4183-4191
- [70] Zhang W, Yu Z, Chen Z, Li M. Preparation of super-hydrophobic Cu/Ni coating with micro-nano hierarchical structure. *Materials Letters*. 2012;**67**:327-330
- [71] Jain R, Pitchumani R. Facile fabrication of durable copper-based superhydrophobic surfaces via electrodeposition. *Langmuir*. 2017;**34**:3159-3169
- [72] Xiang M, Jiang M, Zhang Y, Liu Y, Shen F, Yang G, et al. Fabrication of a novel superhydrophobic and superoleophilic surface by one-step electrodeposition method for continuous oil/water separation. *Applied Surface Science*. 2018;**434**:1015-1020
- [73] Su F, Yao K. Facile fabrication of superhydrophobic surface with excellent mechanical abrasion and corrosion resistance on copper substrate by a novel method. *ACS Applied Materials & Interfaces*. 2014;**6**:8762-8770
- [74] Wu X, Zheng L, Wu D. Fabrication of superhydrophobic surfaces from microstructured ZnO-based surfaces via a wet-chemical route. *Langmuir*. 2005;**21**:2665-2667
- [75] Wu Y, Jia S, Wang S, Qing Y, Yan N, Wang Q, et al. A facile and novel emulsion for efficient and convenient fabrication of durable superhydrophobic materials. *Chemical Engineering Journal*. 2017;**328**:186-196
- [76] Kwon Y, Patankar N, Choi J, Lee J. Design of surface hierarchy for extreme hydrophobicity. *Langmuir*. 2009;**25**:6129-6136
- [77] Choi Y-W, Han J-E, Lee S, Sohn D. Preparation of a superhydrophobic film with UV imprinting technology. *Macromolecular Research*. 2009;**17**:821-824
- [78] Zheng B, Tice JD, Ismagilov RF. Formation of arrayed droplets by soft lithography and two-phase fluid flow, and application in protein crystallization. *Advanced Materials*. 2004;**16**:1365-1368
- [79] Lai Y, Huang Y, Wang H, Huang J, Chen Z, Lin C. Selective formation of ordered arrays of octacalcium phosphate ribbons on TiO<sub>2</sub> nanotube surface by template-assisted electrodeposition. *Colloids and Surfaces B: Biointerfaces*. 2010;**76**:117-122
- [80] Bormashenko E, Stein T, Whyman G, Bormashenko Y, Pogreb R. Wetting properties of the multiscaled nanostructured polymer and metallic superhydrophobic surfaces. *Langmuir*. 2006;**22**:9982-9985
- [81] Cho WK, Choi IS. Fabrication of hairy polymeric films inspired by geckos: Wetting and high adhesion properties. *Advanced Functional Materials*. 2008;**18**:1089-1096
- [82] Yan Y, Gao N, Barthlott W. Mimicking natural superhydrophobic surfaces and grasping the wetting process: A review on recent progress in preparing superhydrophobic surfaces. *Advances in Colloid and Interface Science*. 2011;**169**:80-105
- [83] Borrás A, Barranco A, González-Elipé AR. Reversible superhydrophobic to superhydrophilic conversion of Ag@TiO<sub>2</sub> composite nanofiber surfaces. *Langmuir*. 2008;**24**:8021-8026

- [84] Jung YC, Bhushan B. Mechanically durable carbon nanotube-composite hierarchical structures with superhydrophobicity, self-cleaning, and low-drag. *ACS Nano*. 2009;**3**:4155-4163
- [85] Bravo J, Zhai L, Wu Z, Cohen RE, Rubner MF. Transparent superhydrophobic films based on silica nanoparticles. *Langmuir*. 2007;**23**:7293-7298
- [86] Lee D, Rubner MF, Cohen RE. All-nanoparticle thin-film coatings. *Nano Letters*. 2006;**6**:2305-2312
- [87] Sun C, Ge L-Q, Gu Z-Z. Fabrication of super-hydrophobic film with dual-size roughness by silica sphere assembly. *Thin Solid Films*. 2007;**515**:4686-4690
- [88] Min W-L, Jiang P, Jiang B. Large-scale assembly of colloidal nanoparticles and fabrication of periodic subwavelength structures. *Nanotechnology*. 2008;**19**:475604
- [89] Ma M, Hill RM, Lowery JL, Fridrikh SV, Rutledge GC. Electrospun poly (styrene-block-dimethylsiloxane) block copolymer fibers exhibiting superhydrophobicity. *Langmuir*. 2005;**21**:5549-5554
- [90] Tuteja A, Choi W, Ma M, Mabry JM, Mazzella SA, Rutledge GC, et al. Designing superoleophobic surfaces. *Science*. 2007;**318**:1618-1622
- [91] Ma M, Mao Y, Gupta M, Gleason KK, Rutledge GC. Superhydrophobic fabrics produced by electrospinning and chemical vapor deposition. *Macromolecules*. 2005;**38**:9742-9748
- [92] Mizukoshi T, Matsumoto H, Minagawa M, Tanioka A. Control over wettability of textured surfaces by electrospray deposition. *Journal of Applied Polymer Science*. 2007;**103**:3811-3817
- [93] Zheng J, He A, Li J, Xu J, Han CC. Studies on the controlled morphology and wettability of polystyrene surfaces by electrospinning or electrospraying. *Polymer*. 2006;**47**:7095-7102
- [94] Ding B, Ogawa T, Kim J, Fujimoto K, Shiratori S. Fabrication of a super-hydrophobic nanofibrous zinc oxide film surface by electrospinning. *Thin Solid Films*. 2008;**516**:2495-2501
- [95] Burkarter E, Saul CK, Thomazi F, Cruz NC, Zanata SM, Roman LS, et al. Electrospayed superhydrophobic PTFE: A non-contaminating surface. *Journal of Physics D: Applied Physics*. 2007;**40**:7778
- [96] Li X, Chen G, Ma Y, Feng L, Zhao H, Jiang L, et al. Preparation of a super-hydrophobic poly (vinyl chloride) surface via solvent-nonsolvent coating. *Polymer*. 2006;**47**:506-509
- [97] Nakajima A, Abe K, Hashimoto K, Watanabe T. Preparation of hard super-hydrophobic films with visible light transmission. *Thin Solid Films*. 2000;**376**:140-143
- [98] Shirtcliffe N, McHale G, Newton M, Perry C. Intrinsically superhydrophobic organosilica sol-gel foams. *Langmuir*. 2003;**19**:5626-5631